



## **A central role for intermolecular dityrosine cross-linking of fibrinogen in high molecular weight advanced oxidation protein product (AOPP) formation**

This is the peer reviewed version of the following article:

*Original:*

Colombo, G., Clerici, M., Giustarini, D., Portinaro, N., Badalamenti, S., Rossi, R., et al. (2015). A central role for intermolecular dityrosine cross-linking of fibrinogen in high molecular weight advanced oxidation protein product (AOPP) formation. *BIOCHIMICA ET BIOPHYSICA ACTA-GENERAL SUBJECTS*, 1850(1), 1-12 [10.1016/j.bbagen.2014.09.024].

*Availability:*

This version is available <http://hdl.handle.net/11365/990208> since 2016-03-25T13:12:01Z

*Published:*

DOI:10.1016/j.bbagen.2014.09.024

*Terms of use:*

Open Access

The terms and conditions for the reuse of this version of the manuscript are specified in the publishing policy. Works made available under a Creative Commons license can be used according to the terms and conditions of said license.

For all terms of use and more information see the publisher's website.

(Article begins on next page)

# **A central role for intermolecular dityrosine cross-linking of fibrinogen in high molecular weight advanced oxidation protein product (AOPP) formation**

Graziano Colombo<sup>a1</sup>, Marco Clerici<sup>a,b1</sup>, Daniela Giustarini<sup>c</sup>, Nicola Portinaro<sup>d</sup>, Salvatore Badalamenti<sup>e</sup>, Ranieri Rossi<sup>c</sup>, Aldo Milzani<sup>a</sup>, and Isabella Dalle-Donne<sup>a\*</sup>

<sup>a</sup>Department of Biosciences, Università degli Studi di Milano, Milan, Italy.

<sup>b</sup>Department of Biomedical Sciences for Health, Università degli Studi di Milano, Milan, Italy.

<sup>c</sup>Department of Evolutionary Biology, University of Siena, Siena, Italy.

<sup>d</sup>Clinica ortopedica e traumatologica, Humanitas Clinical and Research Center, Rozzano, Milan, Italy.

<sup>e</sup>Humanitas Clinical and Research Center - Nephrology Unit, Rozzano, Milan, Italy.

*\*Corresponding author at:* Department of Biosciences, University of Milan, via Celoria 26, I-20133 Milan, Italy. Tel.: +39 02 50314792; Fax: +39 02 50314781; E-mail: [quack@unimi.it](mailto:quack@unimi.it)

<sup>1</sup>These authors contributed equally to this work.

*Abbreviations:* AOPPs, advanced oxidation protein products; di-Tyr, dityrosine; DNPH, 2,4-dinitrophenylhydrazine; DTNB, 5,5'-dithiobis(2-nitrobenzoic acid); DTT, dithiotreitol; ECL, enhanced chemiluminescence; HMW, high molecular weight; HOCl, hypochlorous acid; HPLC, high performance (pressure) liquid chromatography; HSA, human serum albumin.

## Abstract

*Background:* Advanced oxidation protein products (AOPPs) are dityrosine cross-linked and carbonyl-containing protein products formed by the reaction of plasma proteins with chlorinated oxidants, such as hypochlorous acid (HOCl). Most studies consider human serum albumin (HSA) the main protein responsible for AOPP formation, although the molecular composition of AOPPs has not yet been elucidated. Here, we investigated the relative contribution of HSA and fibrinogen to generation of AOPPs.

*Methods:* AOPP formation was explored by SDS-PAGE, under both reducing and non-reducing conditions, as well as by analytical gel filtration HPLC coupled to fluorescence detection to determine dityrosine and pentosidine formation.

*Results:* Following exposure to different concentrations of HOCl, HSA resulted to be carbonylated but did not form dityrosine cross-linked high molecular weight aggregates. Differently, incubation of fibrinogen or HSA/fibrinogen mixtures with HOCl at concentrations higher than 150  $\mu$ M induced the formation of pentosidine and high molecular weight (HMW)-AOPPs (> 200 kDa), resulting from intermolecular dityrosine cross-linking. Dityrosine fluorescence increased in parallel with increasing HMW-AOPP formation and increasing fibrinogen concentration in HSA/fibrinogen mixtures exposed to HOCl. This conclusion is corroborated by experiments where dityrosine fluorescence was measured in HOCl-treated human plasma samples containing physiological or supra-physiological fibrinogen concentrations or selectively depleted of fibrinogen, which highlighted that fibrinogen is responsible for the highest fluorescence from dityrosine.

*Conclusions:* A central role for intermolecular dityrosine cross-linking of fibrinogen in HMW-AOPP formation is shown.

*General significance:* These results highlight that oxidized fibrinogen, instead of HSA, is the key protein for intermolecular dityrosine formation in human plasma.

**Keywords:** Advanced oxidation protein products; albumin; fibrinogen; hypochlorous acid; human plasma; dityrosine.

## 1. Introduction

Proteins are the major targets for oxidative damage in vivo because of their relative abundance and their ability to scavenge some reactive species that are generated during oxidative stress. Oxidation

reactions induce modification of amino acid residues, altering the protein structure and function, and can also lead to the formation of protein cross-links and protein fragmentation [1-3]. Accumulation of oxidized protein products increases during the normal ageing process and is causally related to several age-related and/or chronic diseases [1,2,4-7]. A family of plasma oxidized protein compounds, termed 'advanced oxidation protein products' (AOPPs), accumulates in diverse disorders such as diabetes mellitus, metabolic syndrome, atherosclerosis, coronary artery disease, and chronic kidney disease [8-10]. AOPPs are a group of dityrosine-, pentosidine and carbonyl-containing protein products generated by reaction of plasma proteins with hypochlorous acid (HOCl) and chloramines during oxidative stress and generally considered to be carried mainly by albumin in the blood circulation [8,11-13].

Previous studies have identified AOPPs as biomarkers of oxidative damage to proteins and proinflammatory mediators, involved in the activation of both monocytes and polymorphonuclear neutrophils [14] as well as of vascular endothelial cells [15]. Chronic accumulation of AOPPs promotes and worsens inflammation in diabetic kidneys [16] and accelerates atherosclerosis through promoting oxidative stress and inflammation [17]. Furthermore, AOPPs directly impair metabolism of high-density lipoproteins (HDL), being potent HDL receptor antagonists and, therefore, might be directly involved in the development of cardiovascular disease [13]. As AOPPs may contribute to the progression of some human diseases as well as their related complications, monitoring AOPP accumulation could help forecast the progression of some diseases related to oxidative stress. Recent results suggest that strategies aimed at reducing AOPP accumulation could slow the progression of chronic kidney disease [18]. Therefore, AOPPs might also be a potential target for therapeutic intervention.

HOCl generated by the myeloperoxidase-H<sub>2</sub>O<sub>2</sub>-chloride system of activated neutrophils could represent a major pathway for AOPP production, as suggested by in vitro incubation of human plasma with HOCl [11] and by positive correlation between AOPP levels and plasma myeloperoxidase activity in hemodialysis patients [19]. Utilizing indirect techniques, human serum albumin (HSA) was indicated as the main protein contributing to AOPPs in plasma of chronic uremic patients [11]. Some evidence suggests that AOPPs present in plasma of hemodialysis patients consist of two molecular species (as determined by size exclusion chromatography) resulting from the association of several oxidized proteins: high molecular weight (HMW) AOPPs (~600 kDa) were hypothesized to result mainly from HSA aggregates through dityrosine (di-Tyr) cross-linking; low molecular weight AOPPs (~70 kDa) mainly contain HSA and  $\gamma$ -globulins [8,11]. Although in the vast majority of literature AOPP formation is linked to HSA, the molecular composition of AOPPs has not yet been elucidated. Since the AOPP concentration is about 50% [20] or even 300% [21] higher in plasma than in serum (where clotting factors have been removed),

oxidized fibrinogen has been suggested as a key molecule responsible for AOPP formation in human plasma [21,22]. Conversely, another study suggested that plasma fibrinogen is not a component of AOPPs but rather interferes with their measurement [23].

Aim of this study was therefore to evaluate the contribution of HSA and fibrinogen to the *in vitro* formation of dityrosine cross-linked protein aggregates, which in turn could be key for HMW-AOPP formation.

## **2. Materials and methods**

### *2.1 Materials*

Delipidized HSA (~99% agarose gel electrophoresis), 5,5'-dithiobis(2-nitrobenzoic acid) (DTNB), *N*-ethylmaleimide (NEM) and 2,4-dinitrophenylhydrazine (DNPH) were purchased from Sigma-Aldrich (Milan, Italy). Anti-dinitrophenyl-KLH (anti-DNP) antibodies, rabbit IgG fraction and goat anti-rabbit IgG, horseradish peroxidase conjugate were purchased from Molecular Probes (Eugene, OR, USA). ECL Plus Western blotting detection reagents were obtained from GE Healthcare (Milan, Italy). EZ-Link Biotin-HPDP was obtained from Euroclone (Pero, Milan, Italy). All other reagents were of analytical grade (Sigma-Aldrich, Milan, Italy).

### *2.2 Blood collection*

Human blood samples were obtained from healthy donors that voluntarily went to the Analysis Laboratory of University of Milan (Laboratorio Analisi Università di Milano) for a routinary blood analysis, after informed verbal consent. The verbal consent was considered sufficient because the samples were handled anonymously. Human blood was obtained in the morning after 10–12 h of starving from the antecubital vein. Blood samples from uraemic patients undergoing hemodialysis at the Nephrology Unit of the Humanitas Clinical and Research Center (Rozzano, Milan, Italy) were obtained after informed written consent. K<sub>3</sub>EDTA was used as an anticoagulant in all the blood samples.

### *2.3 Purification of human fibrinogen*

Human plasma was obtained centrifuging human blood at 1,000g for 10 min at room temperature. Plasma was incubated at 37°C for 5 min and then centrifuged at 16,000g for 5 min to

pellet eventual precipitates. Fibrinogen was prepared by precipitation of 400  $\mu$ l of plasma with 22% saturated ammonium sulphate [24]. After gently vortexing, sample was centrifuged at 7000g for 5 min to pellet the fibrinogen. The supernatant was discarded and the pellet was washed twice with 1 ml of 25% ammonium sulphate. Finally, fibrinogen pellet was resuspended in 50 mM potassium phosphate buffer (PBS), pH 7.4, and protein concentration was determined by the Bradford assay.

#### *2.4 Preparation of fibrinogen-free, reconstituted and fibrinogen-enriched plasma*

Fibrinogen was precipitated with saturated ammonium sulphate as described above and, after the centrifugation at 7000g for 5 min, the supernatant (fibrinogen-free plasma) was recovered and exhaustively dialysed for 48 h against 50 mM PBS, pH 7.4. After dialysis, the protein content of fibrinogen-free plasma was determined by the Bradford assay. Fibrinogen concentration in human plasma is in the range of 1.5-4.5 mg/ml [25] with a mean concentration of 3 mg/ml. Reconstituted plasma and fibrinogen-enriched plasma were made-up adding, respectively, 3 and 15 mg/ml of purified fibrinogen to fibrinogen-free plasma.

#### *2.5 Preparation of reduced albumin*

Delipidized HSA (12 mg/ml, 0.18 mM) was quantitatively converted to fully reduced HSA (mercaptalbumin), in which the single free thiol (that of Cys34) is completely reduced by treatment with 1.5 mM dithiotreitol (DTT) in 50 mM PBS, pH 7.4, for 15 min, at room temperature. The excess of DTT was then removed by exhaustive dialysis against 50 mM PBS, pH 7.4. HSA concentration was determined by the Bradford assay. In all the experiments with HSA we used fully reduced HSA.

#### *2.6 Protein exposure to HOCl*

In a typical experiment, HSA and fibrinogen were diluted with 50 mM PBS, pH 7.4, to a total final concentration of 1 mg/ml and treated, both individually and as a mixture containing equal amounts of proteins by weight, with various concentrations of HOCl, for 60 min, at 37°C, with gentle rotary shaking. HOCl reactivity was stopped by the addition of a ten-fold molar excess of methionine relative to the highest HOCl concentration. When required, the removal of HOCl and methionine was accomplished by acetone precipitation. Briefly, protein samples were mixed with three volumes of 100% acetone, allowed to precipitate for 30 min at -20°C and then centrifuged at 10,000g for 10 min, at 4°C. Pellets were washed with 70% acetone and re-centrifuged at 10,000g

for 10 min, at 4°C. Finally, dried pellets were re-suspended in 50 mM PBS, pH 7.4 and protein concentration was determined by the Bradford assay.

Normal (control, i.e., human plasma obtained by whole blood added with anticoagulant, as described in sections 2.2 and 2.3), fibrinogen-free, reconstituted, and fibrinogen-enriched plasma (final protein concentration: 1 mg/ml) were subsequently treated with various concentrations of HOCl, for 60 min, at 37°C. HOCl reactivity was stopped by the addition of a ten-fold molar excess of methionine relative to the highest HOCl concentration. Treated samples were separated through size-exclusion HPLC and dityrosine formation was monitored by fluorescence measurements as described below.

### *2.7 Determination of HSA Cys34 free sulfhydryl group by the Ellman assay*

The free thiol concentration of HSA samples (i.e., non-oxidized [control] HSA and HOCl-oxidized HSA samples) was quantified by the Ellman assay [26]. Following exhaustive dialysis against 50 mM PBS, pH 7.4, HSA samples (600 µg in 950 µl) were added with 50 µl of 3 mM DTNB (prepared in 50 mM phosphate buffer, pH 7.4) and incubated for 15 min at 25°C. The free thiol concentration of HSA samples was determined by measuring the increase in absorbance caused by the released TNB anion upon reaction of a thiol with DTNB at 412 nm and using a molar absorption coefficient of  $14.15 \text{ mM}^{-1} \text{ cm}^{-1}$  [27]. The molar concentration of Cys34 thiol was calculated from the molar absorbance of the TNB anion.

### *2.8 Determination of HSA Cys34 free sulfhydryl group by biotin-HPDP binding and Western blot analysis*

HSA samples (i.e., non-oxidized [control] HSA and HOCl-oxidized HSA samples) were mixed with biotin-HPDP (stock solution 4 mM in 90% dimethyl sulfoxide and 10% dimethylformamide) at final molar ratio of 1:7. After mixing by gentle vortexing, the biotinylation reaction was carried out at room temperature in the dark for 60 min, with brief vortex-mixing every 15 min. To remove biotin-HPDP excess, labelled HSA samples were precipitated with acetone and resuspended with an equal volume of 2× non-reducing SDS-PAGE sample buffer. Samples (10 µg total protein) were resolved by SDS-PAGE on 10% Tris-HCl resolving gels, electroblotted to Immobilon P polyvinylidene difluoride (PVDF) membrane and stored at -20°C for later use. To detect biotin-HPDP-labelled HSA Cys34, membranes were blocked for 1 h in 5% (w/v) non-fat dry milk in PBST [10 mM Na-phosphate, pH 7.2, 0.9% (w/v) NaCl, 0.1% (v/v) Tween 20] and probed with horseradish peroxidase (HRP)-conjugated streptavidin (1:5000 dilution) for 2 h in 5% (w/v)

non-fat dry milk in PBST. After washing in PBST, immunoreactive bands were detected by using enhanced chemiluminescence. Protein bands were then visualized by washing the membrane extensively in PBS and staining with Amido black.

### *2.9 Spectrophotometric determination of HSA carbonylation*

Protein carbonyl groups were quantified by adding an equal volume of 10 mM DNPH in 2 M HCl to the different HSA solutions (i.e., non-oxidized [control] HSA and HOCl-oxidized HSA samples). After 1-h incubation in the dark at room temperature, with gentle vortexing every 10 min, samples were precipitated with TCA (20% final concentration) and centrifuged at 13,000g in a tabletop microcentrifuge for 5 min, at room temperature. The supernatants were discarded and HSA pellets were washed once with 20% TCA and at least three times with 1 ml of ethanol/ethylacetate (1:1) to remove any free DNPH. Pellets were finally resuspended in 1 ml of 6 M guanidine hydrochloride (dissolved in 20 mM phosphate buffer, pH 2.3) at 37°C, for 15 min, with vortex mixing. Carbonyl contents were determined from the absorbance at 366 nm using a molar absorption coefficient of 22,000 M<sup>-1</sup> cm<sup>-1</sup> [28].

### *2.10 Determination of HSA carbonylation by Western blot analysis*

Carbonyl groups formed in HOCl-oxidized HSA samples and related control were determined by Western immunoblotting [29-31] after SDS-PAGE separation on 10% (w/v) Tris-HCl polyacrylamide gels of 10 µg total HSA samples and electroblotting to Immobilon P membrane. PVDF membranes were incubated for 5 min in 2 M HCl and for 5 min in DNPH (0.1 mg/ml in 2 M HCl). Subsequently, membranes were washed three times in 2 M HCl and seven times in 100% methanol, 5 min each, followed by one wash in PBST. After blocking the membranes with 5% (wt/vol) non-fat dry milk in PBST for 1 h, carbonyl formation was probed by a 2-h incubation with anti-DNP antibody (1:20,000 dilution) in 5% non-fat dry milk/PBST. After three washes with PBST for 5 min each, membranes were incubated with a 1:60,000 dilution of the HRP-linked secondary antibody in 5% non-fat dry milk/PBST for 1 h. After washing 3 times with PBST for 5 min each, immunostained HSA bands were visualized with enhanced chemiluminescence (ECL). In order to check equal protein loading among different lanes, membranes were finally stained with Amido Black.

### *2.11 Determination of dityrosine*



Dityrosine formation in oxidized samples of HSA, fibrinogen or a mixture of both was evaluated by analytical gel filtration high performance (pressure) liquid chromatography (HPLC) on a BioSep-SEC-S4000 column (300 mm × 7.8 mm) with a guard column (SecurityGuard™ GFC-4000, 4 mm length × 3 mm ID) and UV-VIS detector. Samples were prepared in 50 mM PBS, pH 7.4, at a final concentration of 1 mg/ml. 20 µg was loaded into the column for each sample. The mobile phase consisted of Milli-Q water, containing 0.5% (w/v) SDS and was eluted at 1 ml/min. Eluates were monitored both at 215 nm for measuring absorbance and at 415-nm emission with 325-nm excitation for measuring dityrosine fluorescence [32].

Dityrosine formation in plasma from hemodialyzed patients (n = 35, age range: 45-80) and age-matched healthy control subjects (n = 15) was evaluated by analytical gel filtration HPLC as described above. Plasma samples were diluted 1:15 in 50 mM Tris-HCl, pH 7.4 and 20 µl was loaded into the column for each sample. Eluates were monitored both at 215 nm for measuring protein absorbance and at 415-nm emission with 325-nm excitation for measuring dityrosine fluorescence. In the time range between 6 and 9 min, both the area under the 215-nm absorbance chromatogram and the area under the 415-nm emission fluorescence chromatogram were considered. The ratio between total fluorescence and total absorbance was calculated for each sample.

### *2.12 Determination of pentosidine*

Pentosidine formation in oxidized samples of HSA, fibrinogen or a mixture of both was evaluated by analytical gel filtration HPLC on a BioSep-SEC-S4000 column (300 mm × 7.8 mm) with a guard column (SecurityGuard™ GFC-4000, 4 mm length × 3 mm ID) and UV-VIS detector. Samples were prepared in 50 mM PBS, pH 7.4, at a final concentration of 1 mg/ml. 20 µg was loaded into the column for each sample. The mobile phase consisted of Milli-Q water, containing 0.5% (w/v) SDS and was eluted at 1 ml/min. Eluates were monitored both at 215 nm for measuring absorbance and at 385-nm emission with 335-nm excitation for measuring pentosidine fluorescence [33].

### *2.13 AOPP separation by SDS-PAGE*

AOPPs were separated by SDS-PAGE using 7.5% (w/v) polyacrylamide gels. Protein samples were added to an equal volume of 2× SDS-PAGE sample buffer [60 mM Tris-HCl, pH 6.8, 10% (v/v) glycerol, 2% (w/v) SDS, 0.01% (w/v) bromophenol blue, with (reducing conditions) or without (non-reducing conditions) 5% (w/v) DTT]. Samples were then heated at 95°C for 5 min

before being cooled and loaded onto the gel. Bands were visualized using Coomassie Brilliant Blue staining. Densitometric analysis of the gels was performed using Image J 1.40d software (National Institutes of Health, Bethesda, MD, USA).

#### *2.14 Protein identification by matrix-assisted laser desorption/ionization-time of flight (MALDI-TOF) mass spectrometry (MS) analysis*

Protein bands were manually excised from silver-stained gels and processed as described in our previous paper [31]. One-microliter aliquots of the trypsin-digested protein supernatant were used for MS analysis on a Autoflex MALDI-TOF (Bruker) mass spectrometer. Spectra were accumulated for over a mass range of 700–4000 Da. Alkylation of cysteine by carbamidomethylation and oxidation of methionine were considered as fixed and variable modifications, respectively. One missed cleavage per peptide was allowed, and a mass tolerance of 0.5 Da was used in all searches. Peptides with masses correspondent to those of trypsin and matrix were excluded from the peak list. Proteins were identified by searching against a comprehensive non-redundant protein database (SwissProt 2014 08) using MASCOT programs via the internet [31].

### **3. Results**

#### *3.1 HOCl-induced oxidation of HSA*

HSA is a single polypeptide of 585 amino acids (66.5-kDa), including 18 tyrosine residues and 35 cysteine residues forming 17 intramolecular disulphide bonds, with the only free sulfhydryl group located at Cys34 [34]. When HSA samples (1 mg/ml, i.e. 15  $\mu$ M) were incubated with increasing concentrations of HOCl (ranging from 15 to 1500  $\mu$ M), the number of sulfhydryl groups, as determined by reaction with DTNB, drastically decreased from about 0.9 mol -SH/mol HSA to almost 0 mol -SH/mol HSA (Fig. 1A). Cys34 thiol oxidation was further established in a complementary experiment by using a biotin-based tagging technique, which have been applied with success to monitor the oxidation of protein -SH by reactive oxygen species [35,36]. The biotin tag can be detected at a level of sensitivity in the picomole range using immunoblotting with HRP-conjugated streptavidin. The loss of the biotin signal is proportional to the degree of thiol modification. Drastic oxidation of HSA Cys34 free sulfhydryl group by HOCl was confirmed by biotin-HPDP binding and Western blot analysis (Fig. 1B).

The extent of carbonyl-group formation in HSA exposed to HOCl, quantified by using the spectrophotometric DNPH assay, is shown in Fig. 1C. Increasing HOCl concentrations induced a progressive increase in HSA carbonylation, which was also determined by SDS-PAGE followed by immunoblotting using specific anti-DNP antibodies (Fig. 1D). Furthermore, levels of the cross-linked product dityrosine (di-Tyr) were increased, as assessed by fluorescence (Fig. 4D), only up to 2.5-fold at the highest HOCl concentration (i.e., 1500  $\mu$ M).

### *3.2 HOCl-induced high molecular weight protein aggregates, under reducing and non-reducing conditions, in HSA, fibrinogen or HSA/fibrinogen solutions*

Fibrinogen is a 340 kDa plasma glycoprotein and the precursor to fibrin, which is the primary structural component of blood clots. Fibrinogen is composed of three pairs of different polypeptide chains termed A $\alpha$  (66 kDa), B $\beta$  (54 kDa) and  $\gamma$  (48 kDa). These chains are connected by 29 disulphide bonds, forming a dimeric molecule (A $\alpha$  B $\beta$   $\gamma$ )<sub>2</sub>, with no free sulfhydryl groups [37]. Fig. 3A shows a representative sample of isolated fibrinogen, prepared as described in Materials and Methods and HSA, separated by SDS-PAGE under reducing and non-reducing conditions and stained for total protein with Coomassie blue. We also performed some preliminary experiments with commercial fibrinogen from human plasma (cod. F4883, Sigma-Aldrich), which is bound to a minor amount of plasma interfering compounds than our human plasma-derived fibrinogen preparations (Fig. 2A). We have identified such fibrinogen-associated molecules in our plasma-derived fibrinogen preparations using MALDI-TOF MS (Fig. 2C). According to SDS-PAGE patterns, they resulted to be similar in both fibrinogen preparations, although quantitatively different, i.e., about 7% and 13% of the total protein amount in commercial fibrinogen and our fibrinogen preparation, respectively, as determined by densitometry on SDS-PAGE gel lanes. However, following treatment with HOCl, commercial human fibrinogen gave results comparable to those we obtained with our fibrinogen solutions (see, as an example, Fig. 2B). All the successive experiments were then performed using fibrinogen purified from human plasma as described in Materials and Methods.

Samples of non-oxidized and HOCl-treated HSA (1 mg/ml), fibrinogen (1 mg/ml), and HSA/fibrinogen mixture (both proteins at 0.5 mg/ml) were separated on SDS-PAGE under non-reducing conditions. The exposure of HSA to increasing concentrations of HOCl up to 1500  $\mu$ M did not cause distinct changes in the HSA electrophoretic pattern after SDS-PAGE separation under non-reducing conditions, except for a moderate band disappearance and smear at the highest HOCl concentrations (Fig. 3B). Differently, a marked disappearance of the fibrinogen hexamer band occurred at HOCl concentrations equal or higher than 375  $\mu$ M (Fig. 3B), with an apparent,

concurrent formation of larger aggregates at the highest HOCl concentrations, in particular in HSA/fibrinogen mixture (Fig. 3B).

### *3.3 HOCl-induced formation of dityrosine in HSA, fibrinogen, and HSA/fibrinogen solutions*

Size-exclusion HPLC with fluorometric detection under non-reducing conditions of HSA, fibrinogen, and HSA/fibrinogen mixture exposed to HOCl allowed us to separate HMW protein aggregates resulting from di-Tyr cross-linking (Fig. 4). HOCl induced a very little increase in dityrosine fluorescence emission of HSA samples (Fig. 4D). Differently, HOCl caused a concentration-dependent progressive increase in dityrosine fluorescence in fibrinogen (Fig. 4E) and HSA/fibrinogen samples (Fig. 4F), as highlighted in Fig. 4G, where data are presented as dityrosine fluorescence intensity normalized to the protein concentration, as determined by absorbance at 215 nm (Fig. 4A-C), in the time frame 6-9 min.

As further proof that dityrosine cross-linking is responsible for HMW-AOPP formation, HSA, fibrinogen, and HSA/fibrinogen solutions exposed to HOCl were denatured by heating at 95°C and separated by SDS-PAGE under reducing conditions (Fig. 3C). A progressive increase in HMW-AOPPs was clearly evident in fibrinogen and in HSA/fibrinogen samples exposed to HOCl concentrations higher than 150 µM, whereas no aggregate formation was observed in HSA samples. For the sake of clarity, we define HMW-AOPPs all protein aggregates with molecular weight (very) higher than 200 kDa under reducing conditions. Namely, those that formed a high molecular weight band at the beginning of the running gel (7.5% polyacrylamide) and very large aggregates that did not even enter the stacking gel (4% polyacrylamide) when the samples were run under reducing SDS-PAGE. This experiment demonstrated that HMW-AOPPs are extremely stable and resistant to reduction with DTT and thermal denaturation.

### *3.4 HOCl-induced formation of pentosidine in fibrinogen and HSA/fibrinogen solutions*

In the plasma of chronic uremic patients AOPP levels also correlated with concentration of the advanced glycation end-product (AGE), pentosidine [8,11-13], a stable cross-link between arginine and lysine, which can be detected at very low concentrations based upon its fluorescence properties [33]. We analysed protein bound pentosidine in HSA, fibrinogen, and HSA/fibrinogen mixture exposed to HOCl by means of size-exclusion HPLC with fluorometric detection under non-reducing conditions (Fig. 5). A marked increase in pentosidine fluorescence was detected in fibrinogen and HSA/fibrinogen samples, whereas negligible pentosidine-related fluorescence was measured in HSA samples.

### *3.4 Contribution of fibrinogen in HOCl-induced formation of HMW-AOPPs*

To confirm the key role played by fibrinogen in intermolecular dityrosine cross-linking and, probably, related formation of HMW-AOPPs, control and HOCl-exposed HSA/fibrinogen mixtures containing fibrinogen ranging from 0-100%, and, complementarily, HSA ranging from 100-0% were separated by reducing SDS-PAGE (Fig. 6). Protein samples exposed to 750  $\mu$ M HOCl exhibited a progressive increase in HMW-AOPP content with the increase in fibrinogen concentration (Fig. 6B), whereas control samples did not show any HMW-AOPP formation (Fig. 6A). Densitometric analysis of the Coomassie blue-stained gel highlighted the increase in HMW-AOPP formation with the increase in fibrinogen concentration in HSA/fibrinogen mixtures exposed to HOCl (not shown).

In a parallel experiment, control and HOCl-exposed HSA/fibrinogen mixtures containing 0-100% fibrinogen and, complementarily, 100-0% HSA were separated by size-exclusion HPLC with fluorometric detection under non-reducing conditions (Fig. 7). Protein samples exposed to HOCl clearly exhibited a progressive increase in di-Tyr fluorescence intensity with the increase in fibrinogen concentration (Fig. 7E). In Fig. 7E data are presented as dityrosine fluorescence intensity (Fig. 7D), normalized to protein concentration (as determined by absorbance at 215 nm, Fig. 7B) plotted against protein percentage composition by weight of HSA/fibrinogen mixtures exposed to 750  $\mu$ M HOCl. Differently, protein samples not exposed to HOCl exhibited negligible di-Tyr fluorescence (Fig. 7C). A positive correlation was obtained by plotting the di-Tyr fluorescence intensity normalized to protein concentration shown in Fig. 7E against the content of HMW-AOPPs in corresponding SDS-PAGE bands (as determined by densitometry of Coomassie blue-stained gels) (not shown), indicating that fibrinogen-dependent di-Tyr intermolecular cross-linking is the major contributor to HMW-AOPP formation in HOCl-exposed HSA/fibrinogen mixtures.

### *3.5 Contribution of fibrinogen in HOCl-induced formation of HMW-AOPPs in human plasma*

The contribution of fibrinogen to AOPP formation was also evaluated in human plasma. For this purpose, we prepared different types of plasma: fibrinogen-free plasma, reconstituted plasma, i.e., defibrinogenized plasma added with fibrinogen at physiological concentration, and fibrinogen-enriched plasma, i.e., defibrinogenized plasma added with fibrinogen at a concentration five-fold greater than the physiological one. Control and HOCl-treated human plasma samples, conveniently diluted, were separated by size-exclusion HPLC with fluorometric detection under non-reducing conditions (Fig. 8). Chromatograms obtained from HOCl-treated plasma samples showed that

fibrinogen is the main contributor to di-Tyr fluorescence in normal (Fig. 8E) and reconstituted (Fig. 8G) plasma and that di-Tyr fluorescence is decreased in defibrinogenized plasma (Fig. 8F) compared with normal and reconstituted plasma, whereas it is considerably increased in fibrinogen-enriched plasma (Fig. 8H) compared with normal and reconstituted plasma.

#### 4. Discussion

In the present study, we found that exposure of HSA to HOCl concentrations  $\geq 75 \mu\text{M}$  causes oxidation of more than 90% of its Cys34 thiol (Fig. 1A and B), increasing protein carbonylation (Fig. 1C and D), poor dityrosine formation due to intramolecular cross-linking (Fig. 4D), no dityrosine formation due to intermolecular cross-linking as assessed by reducing SDS-PAGE (Fig. 3C) and no pentosidine formation (Fig. 5). These observations are in agreement with previous studies performed on HOCl-modified albumin [39] or plasma proteins of uremic patients [40,41].

Differently, incubation of fibrinogen or HSA/fibrinogen mixture with HOCl at concentrations higher than  $150 \mu\text{M}$  induced the formation of high molecular weight ( $>200 \text{ kDa}$ ) aggregates, some of which hardly entered the 7.5% polyacrylamide resolving gel and others did not even enter the stacking gel (4% polyacrylamide) (Fig. 3B and C). The concentrations of HOCl *in vivo* are estimated to be 12–250  $\mu\text{M}$  [42]; in particular, HOCl levels in the vicinity of activated neutrophils are at or above  $100 \mu\text{M}$  [43], being estimated to reach as high as 5 mM [44]. As the fibrinogen molecule has no free sulfhydryl groups, whereas it contains 134 tyrosine residues [45], such fibrinogen or HSA/fibrinogen aggregates could be mainly due to dityrosine cross-linking, as also suggested by the presence of such high molecular weight aggregates also when the samples exposed to HOCl concentrations  $\geq 375 \mu\text{M}$  were run under reducing SDS-PAGE (Fig. 3C). Formation of dityrosine in fibrinogen and HSA/fibrinogen samples exposed to HOCl was confirmed by means of size-exclusion HPLC with fluorometric measurement of di-Tyr fluorescence (Fig. 4). Simultaneous disappearance of the three fibrinogen polypeptide chain bands in fibrinogen or HSA/fibrinogen samples exposed to HOCl concentrations higher than  $150 \mu\text{M}$  and electrophoresed under reducing conditions (Fig. 3C) suggests the presence of intermolecular dityrosine cross-links and also supports the concept that oxidized fibrinogen, instead of albumin, is the key protein for intermolecular dityrosine formation, which in turn could be key for HMW-AOPP formation. This hypothesis is backed by the positive correlation between the increase in dityrosine and high molecular weight aggregate formation and the increase in fibrinogen concentration in samples containing a mixture of HSA and fibrinogen, exposed to  $750 \mu\text{M}$  HOCl (Figs. 6 and 7). Fibrinogen susceptibility to intermolecular di-Tyr linkages *in vitro* is supported by previous studies where the protein was exposed to peroxynitrite [46] or to metal ion-catalyzed oxidation [47]. In samples containing HOCl-

exposed HSA/fibrinogen mixtures, the intensity of di-Tyr fluorescence increases almost linearly as the band intensity of HMW-AOPPs increases (not shown), suggesting a central role for intermolecular di-Tyr cross-linking of fibrinogen in HMW-AOPP formation. This conclusion is corroborated by experiments where di-Tyr fluorescence was measured in HOCl-treated plasma samples containing physiological or supra-physiological fibrinogen concentrations or selectively depleted of fibrinogen (Fig. 8), which highlighted that fibrinogen is responsible for the highest fluorescence from dityrosine (Fig. 8E, G and H), even though other plasma protein(s) too contribute to it (Fig. 8F). Our findings confirm and extend a previous study, which suggested from indirect evidence that oxidized fibrinogen is a key molecule responsible for AOPP formation in the blood of patients with various peripheral vascular and cardiovascular diseases and, as a consequence, fibrinogen would contribute to  $A_{340}$  under acidic conditions [21,22].

In summary, our study provides in vitro evidence that oxidized fibrinogen may play a key role in HMW-AOPP formation, although the involvement of other protein(s) in HMW-AOPP formation in human plasma cannot be excluded and warrants further investigation. It is also worth considering that plasma fibrinogen is a heterogeneous mixture of fibrinogen variants [48]. For instance, the oxidation status of plasma-derived fibrinogen may be variable related to inter-individual factors, which could influence interaction of fibrinogen variants with delipidized HSA used in our study. However, we always extracted fibrinogen from at least 12-15 plasma samples, which were pooled before extraction and, therefore, we think this reduces at least some inter-individual differences. Indeed, we performed each experiment at least three times, each time purifying a new solution of fibrinogen from pooled samples of human plasma, obtaining similar results. On the other hand, albumin isolated from blood serum or plasma is usually heterogeneous, mainly because of the variable extent of oxidation of the Cys-34 thiol group and variations in the number and types of bound fatty acids. In the present work, we have therefore used commercial delipidized HSA that we converted to fully reduced HSA, in which the single free thiol of Cys34 is completely reduced. Moreover, cross-link formation of HOCl-treated HSA independent of dityrosine formation was recently described in a study showing irreversible inhibition of the HDL receptor, scavenger receptor class B, type 1, promoted by covalent cross-linking of HOCl-oxidized HSA (i.e., the so-called AOPP-albumin) via *N*-chloramines formed within lysine residues [49]. Conversion of positively charged  $\epsilon$ -amino groups of lysine residues by HOCl results in loss of positive charge through formation of *N*-chloramines. In our samples, chloramine generation was likely mostly reversed by addition of free methionine to HOCl-treated samples to stop HOCl reactivity. However, the possibility that other types of covalent cross-links, besides dityrosine formation, may contribute to HMW-AOPP formation in human plasma cannot be excluded and warrants further investigation.

The development of validated biomarkers for human diseases is essential to improve diagnosis and accelerate the development of new therapies. The collection of small blood volumes is mostly unproblematic and non-invasive biomarkers deliver an advantage over more invasive biomarkers. Because of their ease of determination, by taking advantage of their absorbance at 340 nm under acidic conditions, and stability (AOPPs remained stable during sample storage both at -20°C and -80°C for about six months [38]), increased plasma level of AOPPs is used as an economic indicator of oxidative stress in many diseases, amongst which chronic kidney disease [11,50], inflammatory bowel disease [51], coronary artery disease [9], idiopathic Parkinson's disease [52], and metabolic syndrome [53]. Unfortunately, hemolysis, blood-sampling under non-fasting conditions, high triglycerides, and freeze/thaw cycles can markedly interfere with AOPP measurement, mainly because of sample turbidity following lipid precipitation in plasma samples [11,20]. An additional step that includes precipitation of triglycerides and esterified cholesterol in the form of VLDL and LDL reduces, but does not solve, the turbidity problem [54]. A further improved method that uses citric acid to solubilize plasma lipids before absorbance measurement seems to detect AOPPs with better reproducibility and accuracy compared to previously reported methods [55].

Another problem, strictly related to poor reproducibility and accuracy of most current colorimetric methods for AOPP detection, is the lack of reliable, validated AOPP reference values in healthy humans: reported AOPP concentrations in healthy humans range from  $29.4 \pm 4.9 \mu\text{M}$  to  $170.9 \pm 101.9 \mu\text{M}$  [22]. The recently developed method that uses citric acid as the solvent [55] should allow a more accurate measure of chromophore absorption at 340 nm and, therefore, could help determine reliable AOPP reference values in healthy subjects. However, measuring AOPPs in diluted plasma as absorbance at 340 nm is a rather non-selective way to determine the level of oxidized proteins. It is thus necessary to take precautions to minimize the contribution of species other than AOPPs. In this respect, determination of dityrosine in AOPPs by HPLC with fluorometric detection could be used, in addition to the above-mentioned method, for further studies in order to clarify the role of AOPPs in human disease. To this end, preliminary results from analysis of plasma samples taken from uraemic patients undergoing hemodialysis by size-exclusion HPLC with fluorometric detection show a marked ( $p < 0.001$ ) increase in dityrosine fluorescence (normalized to protein concentration) as compared to healthy controls (Fig. 9).

### **Conflict of interest statement**

The authors declare no conflicts of interest.



## Acknowledgments

This research was supported by Fondazione Ariel ([www.fondazioneariel.it](http://www.fondazioneariel.it)), Rozzano (MI), Italy. The authors are grateful to Dr. Barbara Ponzini and all the personnel at the Analysis Laboratory, Department of Pathophysiology and Transplantation, University of Milan, for their invaluable support in providing blood samples from healthy subjects.

## References

- [1] Dalle-Donne I, Scaloni A, Giustarini D, Cavarra E, Tell G, Lungarella G, Colombo R, Rossi R, Milzani A. Proteins as biomarkers of oxidative/nitrosative stress in diseases: The contribution of redox proteomics. *Mass Spectrom. Rev.* 2005; **24**:55–99.
- [2] Dalle-Donne I, Rossi R, Colombo R, Giustarini D, Milzani A. Biomarkers of oxidative damage in human disease. *Clin. Chem.* 2006; **52**:601-623.
- [3] Bachi A, Dalle-Donne I, Scaloni A. Redox proteomics: Chemical principles, methodological approaches and biological/biomedical promises. *Chem. Rev.* 2013; **113**:596–698.
- [4] Levine R.L., Stadtman E.R. Oxidative modification of proteins during aging. *Exp. Gerontol.* 2001; **36**:1495–1502.
- [5] Rossi R, Giustarini D, Milzani A, Dalle-Donne I. Cysteinylation and homocysteinylation of plasma protein thiols during ageing of healthy human beings. *J. Cell. Mol. Med.* 2009; **13**:3131-3140.
- [6] Dalle-Donne I, Aldini G, Carini M, Colombo R, Rossi R, Milzani A. Protein carbonylation, cellular dysfunction, and disease progression. *J. Cell. Mol. Med.* 2006; **10**:389-406.
- [7] Baraibar M.A., Liu L., Ahmed E.K., Friguet B. Protein oxidative damage at the crossroads of cellular senescence, aging, and age-related diseases. *Oxid. Med. Cell Longev.* 2012; **2012**:919832.
- [8] Witko-Sarsat V., Friedlander M., Capeillere-Blandin C., Nguyen-Khoa T., Nguyen A.T., Zingraff J., Jungers P., Descamps-Latscha B. Advanced oxidation protein products as a novel marker of oxidative stress in uremia. *Kidney Int.* 1996; **49**:1304–1313.
- [9] Barsotti A., Fabbi P., Fedele M., Garibaldi S., Balbi M., Bezante G.P., Risso D., Indiveri F., Ghigliotti G., Brunelli C. Role of advanced oxidation protein products and thiol ratio in patients with acute coronary syndromes. *Clin. Biochem.* 2011; **44**:605-611.
- [10] Colombo G., Clerici M., Giustarini D., Gagliano N., Rossi R., Milzani A., Dalle-Donne I. Redox albuminomics: oxidized albumin in human diseases. *Antioxid. Redox Signal.* 2012; **17**:1515-1527.

- [11] Capeillère-Blandin C., Gausson V., Descamps-Latscha B., Witko-Sarsat V. Biochemical and spectrophotometric significance of advanced oxidized protein products. *Biochim. Biophys. Acta* 2004; **1689**:91–102.
- [12] Capeillère-Blandin C., Gausson V., Nguyen A.T., Descamps-Latscha B., Drueke T., Witko-Sarsat V. Respective role of uremic toxins and myeloperoxidase in the uremic state. *Nephrol. Dial. Transplant.* 2006; **21**:1555–1563.
- [13] Marsche G., Frank S., Hrzanjak A., Holzer M., Dirnberger S., Wadsack C., Scharnagl H., Stojakovic T., Heinemann A., Oetl K. Plasma-Advanced Oxidation Protein Products are potent high-density lipoprotein receptor antagonists in vivo. *Circ. Res.* 2009; **104**:750-757.
- [14] Witko-Sarsat V., Gausson V., Nguyen A.T., Touam M., Drueke T., Santangelo F., Descamps-Latscha B. AOPP-induced activation of human neutrophil and monocyte oxidative metabolism: a potential target for N-acetylcysteine treatment in dialysis patients. *Kidney Int.* 2003; **64**:82–91.
- [15] Guo Z.J., Niu H.X., Hou F.F., Zhang L., Fu N., Nagai R., Lu X., Chen B.H., Shan Y.X., Tian J.W., Nagaraj R.H., Xie D., Zhang X. Advanced oxidation protein products activate vascular endothelial cells via a RAGE-mediated signaling pathway. *Antioxid. Redox Signal.* 2008; **10**:1699–1712.
- [16] Shi X.Y., Hou F.F., Niu H.X., Wang G.B., Xie D., Guo Z.J., Zhou Z.M., Yang F., Tian J.W., Zhang X. Advanced oxidation protein products promote inflammation in diabetic kidney through activation of renal nicotinamide adenine dinucleotide phosphate oxidase. *Endocrinology* 2008; **149**:1829–1839.
- [17] Liu S.X., Hou F.F., Guo Z.J., Nagai R., Zhang W.R., Liu Z.Q., Zhou Z.M., Zhou M., Xie D., Wang G.B., Zhang X. Advanced oxidation protein products accelerate atherosclerosis through promoting oxidative stress and inflammation. *Arterioscler. Thromb. Vasc. Biol.* 2006; **26**:1156–1162.
- [18] Cao W., Xu J., Zhou Z.M, Wang G.B., Hou F.F., Nie J. Advanced Oxidation Protein Products activate intrarenal renin–angiotensin system via a CD36-mediated, redox-dependent pathway. *Antioxid. Redox Signal.* 2013; **18**:19–35.
- [19] Rodriguez-Ayala E., Anderstam B., Suliman M.E., Seeberger A., Heimbürger O., Lindholm B., Stenvinkel P. Enhanced RAGE-mediated NF- $\kappa$ B stimulation in inflamed hemodialysis patients. *Atherosclerosis* 2005; **180**:333–340.
- [20] Valli A., Suliman M.E., Meert N., Vanholder R., Lindholm B., Stenvinkel P., Watanabe M., Barany P., Alvestrand A., Anderstam B. Overestimation of advanced oxidation protein products in uremic plasma due to presence of triglycerides and other endogenous factors. *Clin. Chim. Acta* 2007; **379**:87–94.

- [21] Selmeçi L., Székely M., Soós P., Seres L., Klinga N., Geiger A., Acsády G. Human blood plasma advanced oxidation protein products (AOPP) correlates with fibrinogen levels. *Free Radic. Res.* 2006; **40**:952–958.
- [22] Selmeçi L. Advanced oxidation protein products (AOPP): novel uremic toxins, or components of the non-enzymatic antioxidant system of the plasma proteome? *Free Radic. Res.* 2011; **45**:1115–1123.
- [23] Chen Y.H., Shi W., Liang X.L., Liang Y.Z., Fu X. Effect of blood sample type on the measurement of advanced oxidation protein products as a biomarker of inflammation and oxidative stress in hemodialysis patients. *Biomarkers* 2011; **16**:129-135.
- [24] Paton L.N., Mocatta T.J., Richards A.M., Winterbourn C.C. Increased thrombin-induced polymerization of fibrinogen associated with high protein carbonyl levels in plasma from patients post myocardial infarction. *Free Radic. Biol. Med.* 2010; **48**:223-229.
- [25] Lowe G.D., Rumley A., Mackie I.J. Plasma fibrinogen. *Ann. Clin. Biochem.* 2004; **41**:430-440.
- [26] Ellman G.L. Tissue sulfhydryl groups. *Arch. Biochem. Biophys.* 1959; **82**:70–77.
- [27] Riddles P.W., Blakeley R.L., Zerner B. Reassessment of Ellman's reagent. *Methods Enzymol.* 1983; **91**:49–60.
- [28] Levine R.L., Williams J.A., Stadtman E.R., Shacter E. Carbonyl assays for determination of oxidatively modified proteins. *Methods Enzymol.* 1994; **233**:346–357.
- [29] Dalle-Donne I., Carini M., Vistoli G., Gamberoni L., Giustarini D., Colombo R., Maffei Facino R., Rossi R., Milzani A., Aldini G. Actin Cys374 as a nucleophilic target of alpha,beta-unsaturated aldehydes. *Free Radic. Biol. Med.* 2007; **42**:583–598.
- [30] Colombo G., Aldini G., Orioli M., Giustarini D., Gornati R., Rossi R., Colombo R., Carini M., Milzani A., Dalle-Donne I. Water-Soluble alpha,beta-unsaturated aldehydes of cigarette smoke induce carbonylation of human serum albumin. *Antioxid. Redox Signal.* 2010; **12**:349-364.
- [31] Colombo G., Dalle-Donne I., Orioli M., Giustarini D., Rossi R., Carini M., Aldini G., Milzani A., Butterfield D.A., Gagliano N. Oxidative damage in human gingival fibroblasts exposed to cigarette smoke. *Free Radic. Biol. Med.* 2012; **52**:1584-1596.
- [32] Dalle-Donne I., Rossi R., Giustarini D., Gagliano N., Lusini L., Milzani A., Di Simplicio P., Colombo R. Actin carbonylation: from a simple marker of protein oxidation to relevant signs of severe functional impairment. *Free Radic. Biol. Med.* 2001; **31**:1075–1083.
- [33] Sell DR, Monnier VM. Structure elucidation of a senescence cross-link from human extracellular matrix. Implication of pentoses in the aging process. *J. Biol. Chem.* 1989; **264**:21597-21602.

- [34] Carballal S., Alvarez B., Turell L., Botti H., Freeman B.A., Radi R. Sulfenic acid in human serum albumin. *Amino Acids* 2007; **32**:543-551.
- [35] Landar A., Oh J.Y., Giles N.M., Isom A., Kirk M., Barnes S., Darley-Usmar V.M. A sensitive method for the quantitative measurement of protein thiol modification in response to oxidative stress. *Free Radic. Biol. Med.* 2006; **40**:459-468.
- [36] Colombo G., Rossi R., Gagliano N., Portinaio N., Clerici M., Annibal A., Giustarini D., Colombo R., Milzani A., Dalle-Donne I. Red blood cells protect albumin from cigarette smoke-induced oxidation. *PLoS ONE* 2012; **7**:e29930.
- [37] Herrick S., Blanc-Brude O., Gray A., Laurent G. Fibrinogen. *Int. J. Biochem. Cell. Biol.* 1999; **31**:741-746.
- [38] Matteucci E., Biasci E., Giampietro O. Advanced oxidation protein products in plasma: stability during storage and correlations with other clinical characteristics. *Acta Diabetol.* 2001; **38**:187-189.
- [39] Fu S., Wang H., Davies M., Dean R. Reactions of hypochlorous acid with tyrosine and peptidyl-tyrosyl residues give dichlorinated and aldehydic products in addition to 3-chlorotyrosine. *J. Biol. Chem.* 2000; **75**:10851-10858.
- [40] Himmelfarb J., McMonagle E., McMenemy E. Plasma protein thiol oxidation and carbonyl formation in chronic renal failure. *Kidney Int.* 2000; **58**:2571-2578.
- [41] Himmelfarb J., McMonagle E. Albumin is the major plasma protein target of oxidant stress in uremia. *Kidney Int.* 2001; **60**:358-563.
- [42] McCall M.R., Carr A.C., Forte T.M., Frei B. LDL modified by hypochlorous acid is a potent inhibitor of lecithin-cholesterol acyltransferase activity. *Arterioscler. Thromb. Vasc. Biol.* 2001; **21**:1040-1045.
- [43] Foote, C.S., Goyne, T.E., Lehrer, R.I. Assessment of chlorination by human neutrophils. *Nature* 1983; **301**:715-716.
- [44] Weiss S.J. Tissue destruction by neutrophils. *N. Engl. J. Med.* 1989; **320**:365-376.
- [45] Mosesson M.W. Fibrinogen structure and fibrin clot assembly. *Semin. Thromb. Hemost.* 1998; **24**:169-174.
- [46] Nowak P., Zbikowska H.M., Ponczek M., Kolodziejczyk J., Wachowicz B. Different vulnerability of fibrinogen subunits to oxidative/nitrative modifications induced by peroxynitrite: functional consequences. *Thromb. Res.* 2007; **121**:163-174.
- [47] Tetik S., Kaya K., Demir M., Eksioğlu-Demiralp E., Yardimci T. Oxidative modification of fibrinogen affects its binding activity to glycoprotein (GP) IIb/IIIa. *Clin. Appl. Thromb. Hemost.* 2010; **16**:51-59.

- [48] de Maat M.P., Verschuur M. Fibrinogen heterogeneity: inherited and noninherited. *Curr. Opin. Hematol.* 2005; **12**:377-383.
- [49] Binder V., Ljubojevic S., Haybaeck J., Holzer M., El-Gamal D., Schicho R., Pieske B., Heinemann A., Marsche G. The myeloperoxidase product hypochlorous acid generates irreversible high-density lipoprotein receptor inhibitors. *Arterioscler. Thromb. Vasc. Biol.* 2013; **33**:1020-1027.
- [50] Mayer B., Zitta S., Greilberger J., Holzer H., Reibnegger G., Hermetter A., Oetl K. Effect of hemodialysis on the antioxidative properties of serum. *Biochim. Biophys. Acta* 2003; **1638**:267–272.
- [51] Krzystek-Korpacka M., Neubauer K., Berdowska I., Boehm D., Zielinski B., Petryszyn P., Terlecki G., Paradowski L., Gamian A. Enhanced formation of advanced oxidation protein products in IBD. *Inflamm. Bowel Dis.* 2008; **14**:794-802.
- [52] García-Moreno J.M., Martín de Pablos A., García-Sánchez M.I., Méndez-Lucena C., Damas-Hermoso F., Rus M., Chacón J., Fernández E. May serum levels of advanced oxidized protein products serve as a prognostic marker of disease duration in patients with idiopathic Parkinson's disease? *Antioxid. Redox Signal.* 2013; **18**:1296-1302.
- [53] Korkmaz G.G., Altnoglu E., Civelek S., Sozer V., Erdenen F., Tabak O., Uzun H. The association of oxidative stress markers with conventional risk factors in the metabolic syndrome. *Metabolism* 2013; **62**:828-835.
- [54] Anderstam B., Bragfors-Helin A.C., Valli A., Stenvinkel P., Lindholm B., Suliman M.E. Modification of the oxidative stress biomarker AOPP assay: application in uremic samples. *Clin. Chim. Acta* 2008; **393**:114–118.
- [55] Hanasand M., Omdal R., Norheim K.B., Gøransson L.G., Brede C., Jonsson G. Improved detection of advanced oxidation protein products in plasma. *Clin. Chim. Acta* 2012; **413**:901-906.

## Figure legends

**Fig. 1.** HOCl-induced oxidation of HSA. (A,B) Effect of HOCl on HSA Cys34 sulfhydryl group as determined (A) by the Ellman assay and (B) by biotin-HPDP binding and Western blot analysis. (C,D) Effect of HOCl on HSA carbonylation. (C) Carbonyl formation was assessed from the absorbance at 366 nm after protein derivatization with DNPH. (D) The increase in HSA carbonyl

content was also analysed using reducing SDS-PAGE/Western blotting probed with anti-DNP antibodies. Data are presented as the mean  $\pm$  SD for three independent experiments. Immunoblots show representative images of three independent experiments.

**Fig. 2.** Electrophoretic patterns of commercial and our ammonium sulphate precipitated preparations of human fibrinogen. (A) Representative samples of commercial fibrinogen (CF) and our plasma-derived fibrinogen obtained by ammonium-sulphate precipitation (ASF) separated by SDS-PAGE (10% Tris-HCl resolving gels) under reducing conditions. The relative percentage of each polypeptide chain (P1, ... P12) to the total protein amount is indicated on the right. Molecular weight markers are indicated on the left. (B) Electrophoretic patterns (10% Tris-HCl resolving gels), under reducing conditions, of commercial and our ammonium sulphate precipitated preparations of human fibrinogen exposed to HOCl. (C) Identification, by MALDI-TOF MS analysis, of the main plasma interfering compounds present in our fibrinogen preparations. Protein bands were visualized by staining with Coomassie Blue G250. Representative gels of three independent experiments are shown.

**Fig. 3.** Electrophoretic patterns, under reducing and non-reducing conditions, of HSA, fibrinogen or HSA/fibrinogen mixtures containing 50% HSA and 50% fibrinogen by weight, exposed to HOCl. (A) Representative samples of isolated HSA and human fibrinogen prepared as described under Materials and Methods and separated by SDS-PAGE (10% Tris-HCl resolving gels) under reducing (with DTT) and non-reducing (without DTT) conditions; fibrinogen A $\alpha$  (66 kDa), B $\beta$  (54 kDa), and  $\gamma$  (48 kDa) chains are marked. Approximately 8  $\mu$ g of proteins were applied to each lane. (B) Samples of native and HOCl-treated HSA, fibrinogen and HSA/fibrinogen mixtures were separated by SDS-PAGE under non-reducing conditions. (C) Samples of native and HOCl-treated HSA, fibrinogen and HSA/fibrinogen mixtures were separated by SDS-PAGE under reducing conditions. In both (B) and (C), approximately 8  $\mu$ g of HSA or fibrinogen were applied to each lane, whereas approximately 16  $\mu$ g of HSA/fibrinogen mixtures were applied to each lane; the lane on the left shows high molecular weight protein markers. Protein bands were visualized by staining with Coomassie Blue R250. Representative gels of three independent experiments are shown.

**Fig. 4.** Determination of dityrosine in HSA, fibrinogen, and HSA/fibrinogen mixtures containing 50% HSA and 50% fibrinogen by weight, exposed to HOCl, by size-exclusion HPLC with fluorometric detection. HPLC profiles of (A and D) HSA, (B and E) fibrinogen, and (C and F) HSA/fibrinogen mixtures; protein samples were exposed to 15-1500  $\mu$ M HOCl but, for simplicity, only chromatograms relative to controls (solid line) and samples exposed to 375  $\mu$ M (dotted line) or

1500  $\mu\text{M}$  (dashed line) HOCl are shown. Eluates were monitored for absorbance at 215 nm to measure protein concentration (A-C) and for fluorescence with  $\lambda_{\text{ex}}$  at 325 nm and  $\lambda_{\text{em}}$  at 415 nm to measure di-Tyr fluorescence (D-F). In E and F, arrow indicates the di-Tyr fluorescence peak of HMW-AOPPs. Representative chromatograms of three independent experiments are shown. (G) Dityrosine fluorescence intensity at  $\lambda_{\text{em}} = 415$  nm (D-F) normalized to the protein concentration, as determined by absorbance at 215 nm (A-C) (calculated for the peak area in the time frame 6-9 min), was plotted versus HOCl concentrations for HSA (dotted line), fibrinogen (solid line), and HSA/fibrinogen mixtures (dashed line). Data are presented as the mean  $\pm$  SD for three independent measurements.

**Fig. 5.** Determination of pentosidine in HSA, fibrinogen, and HSA/fibrinogen mixtures containing 50% HSA and 50% fibrinogen by weight, exposed to HOCl, by size-exclusion HPLC with fluorometric detection. Eluates were monitored for absorbance at 215 nm to measure protein concentration and for fluorescence with  $\lambda_{\text{ex}}$  at 335 and  $\lambda_{\text{em}}$  at 385 nm to measure pentosidine fluorescence. Pentosidine fluorescence intensity normalized to the protein concentration (calculated for the peak area in the time frame 6-9 min) versus HOCl concentration is shown. Data are presented as the mean  $\pm$  SD for three independent measurements.

**Fig. 6.** Electrophoretic pattern, under reducing conditions, of HSA/fibrinogen mixtures, containing fibrinogen ranging from 0–100% and albumin ranging from 100–0%. (A) HSA/fibrinogen mixtures not exposed to HOCl. (B) HSA/fibrinogen mixtures exposed to 750  $\mu\text{M}$  HOCl. In both gels, approximately 8  $\mu\text{g}$  of proteins were applied to each lane. Protein bands were visualized by staining with Coomassie Blue R250. The lane on the left shows high molecular weight protein markers. Representative gels of three independent experiments are shown.

**Fig. 7.** Determination of dityrosine in HSA/fibrinogen mixtures containing fibrinogen ranging from 0–100% and albumin ranging from 100–0%, exposed to 750  $\mu\text{M}$  HOCl, by size-exclusion HPLC with fluorometric detection. (A and C) HSA/fibrinogen mixtures not exposed to HOCl. (B and D) HSA/fibrinogen mixtures exposed to 750  $\mu\text{M}$  HOCl. For simplicity, only chromatograms relative to samples containing 100% HSA/0% fibrinogen (solid line), 0% HSA/100% fibrinogen (dotted line) and 50% HSA/50% fibrinogen (dashed line) are shown. Eluates were monitored for absorbance at 215 nm to measure protein concentration (A and B) and for fluorescence with  $\lambda_{\text{ex}}$  at 325 nm and  $\lambda_{\text{em}}$  at 415 nm to measure di-Tyr fluorescence (C and D). In D, arrow indicates the di-Tyr fluorescence peak of HMW-AOPPs. Representative chromatograms of three independent experiments are shown. (E) Dityrosine fluorescence intensity at  $\lambda_{\text{em}} = 415$  nm of HOCl-treated samples (D) normalized to

the protein concentration, as determined by absorbance at 215 nm (B) (calculated for the peak area in the time frame 6-9 min), was plotted versus protein percentage composition by weight of HSA/fibrinogen mixtures exposed to 750  $\mu\text{M}$  HOCl. Data are presented as the mean  $\pm$  SD for three independent measurements.

**Fig. 8.** Determination of dityrosine in human plasma exposed to HOCl by size-exclusion HPLC with fluorometric detection. HPLC profiles of (A and E) human plasma, (B and F) fibrinogen-free plasma, (C and G) reconstituted plasma, i.e., defibrinogenized plasma added with fibrinogen at physiological concentration, and (D and H) fibrinogen-enriched plasma, i.e., defibrinogenized plasma added with fibrinogen at a concentration five-fold greater than the physiological one. Protein samples were exposed to 375  $\mu\text{M}$  (dotted line) or 1500  $\mu\text{M}$  HOCl (dashed line). Eluates were monitored for absorbance at 215 nm to measure protein concentration (A-D) and for fluorescence with  $\lambda_{\text{ex}}$  at 325 nm and  $\lambda_{\text{em}}$  at 415 nm to measure di-Tyr fluorescence (E-H). Representative chromatograms of three independent experiments are shown.

**Fig. 9.** Determination of dityrosine in human plasma from healthy subjects and hemodialyzed patients by size-exclusion HPLC with fluorometric detection. Eluates were monitored for absorbance at 215 nm to measure protein concentration and for fluorescence with  $\lambda_{\text{ex}}$  at 325 nm and  $\lambda_{\text{em}}$  at 415 nm to measure di-Tyr fluorescence. Significance between the two groups was determined by *t* test.



# **A central role for intermolecular dityrosine cross-linking of fibrinogen in high molecular weight advanced oxidation protein product (AOPP) formation**

Graziano Colombo<sup>a1</sup>, Marco Clerici<sup>a,b1</sup>, Daniela Giustarini<sup>c</sup>, Nicola Portinaro<sup>d</sup>, Salvatore Badalamenti<sup>e</sup>, Ranieri Rossi<sup>c</sup>, Aldo Milzani<sup>a</sup>, and Isabella Dalle-Donne<sup>a\*</sup>

<sup>a</sup>Department of Biosciences, Università degli Studi di Milano, Milan, Italy.

<sup>b</sup>Department of Biomedical Sciences for Health, Università degli Studi di Milano, Milan, Italy.

<sup>c</sup>Department of Evolutionary Biology, University of Siena, Siena, Italy.

<sup>d</sup>Clinica ortopedica e traumatologica, Humanitas Clinical and Research Center, Rozzano, Milan, Italy.

<sup>e</sup>Humanitas Clinical and Research Center - Nephrology Unit, Rozzano, Milan, Italy.

\**Corresponding author at:* Department of Biosciences, University of Milan, via Celoria 26, I-20133 Milan, Italy. Tel.: +39 02 50314792; Fax: +39 02 50314781; E-mail: [quack@unimi.it](mailto:quack@unimi.it)

<sup>1</sup>These authors contributed equally to this work.

*Abbreviations:* AOPPs, advanced oxidation protein products; di-Tyr, dityrosine; DNPH, 2,4-dinitrophenylhydrazine; DTNB, 5,5'-dithiobis(2-nitrobenzoic acid); DTT, dithiotreitol; ECL, enhanced chemiluminescence; HMW, high molecular weight; HOCl, hypochlorous acid; HPLC, high performance (pressure) liquid chromatography; HSA, human serum albumin.

## Abstract

*Background:* Advanced oxidation protein products (AOPPs) are dityrosine cross-linked and carbonyl-containing protein products formed by the reaction of plasma proteins with chlorinated oxidants, such as hypochlorous acid (HOCl). Most studies consider human serum albumin (HSA) the main protein responsible for AOPP formation, although the molecular composition of AOPPs has not yet been elucidated. Here, we investigated the relative contribution of HSA and fibrinogen to generation of AOPPs.

*Methods:* AOPP formation was explored by SDS-PAGE, under both reducing and non-reducing conditions, as well as by analytical gel filtration HPLC coupled to fluorescence detection to determine dityrosine and pentosidine formation.

*Results:* Following exposure to different concentrations of HOCl, HSA resulted to be carbonylated but did not form dityrosine cross-linked high molecular weight aggregates. Differently, incubation of fibrinogen or HSA/fibrinogen mixtures with HOCl at concentrations higher than 150  $\mu$ M induced the formation of pentosidine and high molecular weight (HMW)-AOPPs (> 200 kDa), resulting from intermolecular dityrosine cross-linking. Dityrosine fluorescence increased in parallel with increasing HMW-AOPP formation and increasing fibrinogen concentration in HSA/fibrinogen mixtures exposed to HOCl. This conclusion is corroborated by experiments where dityrosine fluorescence was measured in HOCl-treated human plasma samples containing physiological or supra-physiological fibrinogen concentrations or selectively depleted of fibrinogen, which highlighted that fibrinogen is responsible for the highest fluorescence from dityrosine.

*Conclusions:* A central role for intermolecular dityrosine cross-linking of fibrinogen in HMW-AOPP formation is shown.

*General significance:* These results highlight that oxidized fibrinogen, instead of HSA, is the key protein for intermolecular dityrosine formation in human plasma.

**Keywords:** Advanced oxidation protein products; albumin; fibrinogen; hypochlorous acid; human plasma; dityrosine.

## 1. Introduction

Proteins are the major targets for oxidative damage in vivo because of their relative abundance and their ability to scavenge some reactive species that are generated during oxidative stress. Oxidation

reactions induce modification of amino acid residues, altering the protein structure and function, and can also lead to the formation of protein cross-links and protein fragmentation [1-3]. Accumulation of oxidized protein products increases during the normal ageing process and is causally related to several age-related and/or chronic diseases [1,2,4-7]. A family of plasma oxidized protein compounds, termed 'advanced oxidation protein products' (AOPPs), accumulates in diverse disorders such as diabetes mellitus, metabolic syndrome, atherosclerosis, coronary artery disease, and chronic kidney disease [8-10]. AOPPs are a group of dityrosine-, pentosidine and carbonyl-containing protein products generated by reaction of plasma proteins with hypochlorous acid (HOCl) and chloramines during oxidative stress and generally considered to be carried mainly by albumin in the blood circulation [8,11-13].

Previous studies have identified AOPPs as biomarkers of oxidative damage to proteins and proinflammatory mediators, involved in the activation of both monocytes and polymorphonuclear neutrophils [14] as well as of vascular endothelial cells [15]. Chronic accumulation of AOPPs promotes and worsens inflammation in diabetic kidneys [16] and accelerates atherosclerosis through promoting oxidative stress and inflammation [17]. Furthermore, AOPPs directly impair metabolism of high-density lipoproteins (HDL), being potent HDL receptor antagonists and, therefore, might be directly involved in the development of cardiovascular disease [13]. As AOPPs may contribute to the progression of some human diseases as well as their related complications, monitoring AOPP accumulation could help forecast the progression of some diseases related to oxidative stress. Recent results suggest that strategies aimed at reducing AOPP accumulation could slow the progression of chronic kidney disease [18]. Therefore, AOPPs might also be a potential target for therapeutic intervention.

HOCl generated by the myeloperoxidase-H<sub>2</sub>O<sub>2</sub>-chloride system of activated neutrophils could represent a major pathway for AOPP production, as suggested by in vitro incubation of human plasma with HOCl [11] and by positive correlation between AOPP levels and plasma myeloperoxidase activity in hemodialysis patients [19]. Utilizing indirect techniques, human serum albumin (HSA) was indicated as the main protein contributing to AOPPs in plasma of chronic uremic patients [11]. Some evidence suggests that AOPPs present in plasma of hemodialysis patients consist of two molecular species (as determined by size exclusion chromatography) resulting from the association of several oxidized proteins: high molecular weight (HMW) AOPPs (~600 kDa) were hypothesized to result mainly from HSA aggregates through dityrosine (di-Tyr) cross-linking; low molecular weight AOPPs (~70 kDa) mainly contain HSA and  $\gamma$ -globulins [8,11]. Although in the vast majority of literature AOPP formation is linked to HSA, the molecular composition of AOPPs has not yet been elucidated. Since the AOPP concentration is about 50% [20] or even 300% [21] higher in plasma than in serum (where clotting factors have been removed),

oxidized fibrinogen has been suggested as a key molecule responsible for AOPP formation in human plasma [21,22]. Conversely, another study suggested that plasma fibrinogen is not a component of AOPPs but rather interferes with their measurement [23].

Aim of this study was therefore to evaluate the contribution of HSA and fibrinogen to the *in vitro* formation of dityrosine cross-linked protein aggregates, which in turn could be key for HMW-AOPP formation.

## **2. Materials and methods**

### *2.1 Materials*

Delipidized HSA (~99% agarose gel electrophoresis), 5,5'-dithiobis(2-nitrobenzoic acid) (DTNB), *N*-ethylmaleimide (NEM) and 2,4-dinitrophenylhydrazine (DNPH) were purchased from Sigma-Aldrich (Milan, Italy). Anti-dinitrophenyl-KLH (anti-DNP) antibodies, rabbit IgG fraction and goat anti-rabbit IgG, horseradish peroxidase conjugate were purchased from Molecular Probes (Eugene, OR, USA). ECL Plus Western blotting detection reagents were obtained from GE Healthcare (Milan, Italy). EZ-Link Biotin-HPDP was obtained from Euroclone (Pero, Milan, Italy). All other reagents were of analytical grade (Sigma-Aldrich, Milan, Italy).

### *2.2 Blood collection*

Human blood samples were obtained from healthy donors that voluntarily went to the Analysis Laboratory of University of Milan (Laboratorio Analisi Università di Milano) for a routinary blood analysis, after informed verbal consent. The verbal consent was considered sufficient because the samples were handled anonymously. Human blood was obtained in the morning after 10–12 h of starving from the antecubital vein. Blood samples from uraemic patients undergoing hemodialysis at the Nephrology Unit of the Humanitas Clinical and Research Center (Rozzano, Milan, Italy) were obtained after informed written consent. K<sub>3</sub>EDTA was used as an anticoagulant in all the blood samples.

### *2.3 Purification of human fibrinogen*

Human plasma was obtained centrifuging human blood at 1,000g for 10 min at room temperature. Plasma was incubated at 37°C for 5 min and then centrifuged at 16,000g for 5 min to

pellet eventual precipitates. Fibrinogen was prepared by precipitation of 400  $\mu$ l of plasma with 22% saturated ammonium sulphate [24]. After gently vortexing, sample was centrifuged at 7000g for 5 min to pellet the fibrinogen. The supernatant was discarded and the pellet was washed twice with 1 ml of 25% ammonium sulphate. Finally, fibrinogen pellet was resuspended in 50 mM potassium phosphate buffer (PBS), pH 7.4, and protein concentration was determined by the Bradford assay.

#### *2.4 Preparation of fibrinogen-free, reconstituted and fibrinogen-enriched plasma*

Fibrinogen was precipitated with saturated ammonium sulphate as described above and, after the centrifugation at 7000g for 5 min, the supernatant (fibrinogen-free plasma) was recovered and exhaustively dialysed for 48 h against 50 mM PBS, pH 7.4. After dialysis, the protein content of fibrinogen-free plasma was determined by the Bradford assay. Fibrinogen concentration in human plasma is in the range of 1.5-4.5 mg/ml [25] with a mean concentration of 3 mg/ml. Reconstituted plasma and fibrinogen-enriched plasma were made-up adding, respectively, 3 and 15 mg/ml of purified fibrinogen to fibrinogen-free plasma.

#### *2.5 Preparation of reduced albumin*

Delipidized HSA (12 mg/ml, 0.18 mM) was quantitatively converted to fully reduced HSA (mercaptalbumin), in which the single free thiol (that of Cys34) is completely reduced by treatment with 1.5 mM dithiotreitol (DTT) in 50 mM PBS, pH 7.4, for 15 min, at room temperature. The excess of DTT was then removed by exhaustive dialysis against 50 mM PBS, pH 7.4. HSA concentration was determined by the Bradford assay. In all the experiments with HSA we used fully reduced HSA.

#### *2.6 Protein exposure to HOCl*

In a typical experiment, HSA and fibrinogen were diluted with 50 mM PBS, pH 7.4, to a total final concentration of 1 mg/ml and treated, both individually and as a mixture containing equal amounts of proteins by weight, with various concentrations of HOCl, for 60 min, at 37°C, with gentle rotary shaking. HOCl reactivity was stopped by the addition of a ten-fold molar excess of methionine relative to the highest HOCl concentration. When required, the removal of HOCl and methionine was accomplished by acetone precipitation. Briefly, protein samples were mixed with three volumes of 100% acetone, allowed to precipitate for 30 min at -20°C and then centrifuged at 10,000g for 10 min, at 4°C. Pellets were washed with 70% acetone and re-centrifuged at 10,000g

for 10 min, at 4°C. Finally, dried pellets were re-suspended in 50 mM PBS, pH 7.4 and protein concentration was determined by the Bradford assay.

Normal (control, i.e., human plasma obtained by whole blood added with anticoagulant, as described in sections 2.2 and 2.3), fibrinogen-free, reconstituted, and fibrinogen-enriched plasma (final protein concentration: 1 mg/ml) were subsequently treated with various concentrations of HOCl, for 60 min, at 37°C. HOCl reactivity was stopped by the addition of a ten-fold molar excess of methionine relative to the highest HOCl concentration. Treated samples were separated through size-exclusion HPLC and dityrosine formation was monitored by fluorescence measurements as described below.

### *2.7 Determination of HSA Cys34 free sulfhydryl group by the Ellman assay*

The free thiol concentration of HSA samples (i.e., non-oxidized [control] HSA and HOCl-oxidized HSA samples) was quantified by the Ellman assay [26]. Following exhaustive dialysis against 50 mM PBS, pH 7.4, HSA samples (600 µg in 950 µl) were added with 50 µl of 3 mM DTNB (prepared in 50 mM phosphate buffer, pH 7.4) and incubated for 15 min at 25°C. The free thiol concentration of HSA samples was determined by measuring the increase in absorbance caused by the released TNB anion upon reaction of a thiol with DTNB at 412 nm and using a molar absorption coefficient of  $14.15 \text{ mM}^{-1} \text{ cm}^{-1}$  [27]. The molar concentration of Cys34 thiol was calculated from the molar absorbance of the TNB anion.

### *2.8 Determination of HSA Cys34 free sulfhydryl group by biotin-HPDP binding and Western blot analysis*

HSA samples (i.e., non-oxidized [control] HSA and HOCl-oxidized HSA samples) were mixed with biotin-HPDP (stock solution 4 mM in 90% dimethyl sulfoxide and 10% dimethylformamide) at final molar ratio of 1:7. After mixing by gentle vortexing, the biotinylation reaction was carried out at room temperature in the dark for 60 min, with brief vortex-mixing every 15 min. To remove biotin-HPDP excess, labelled HSA samples were precipitated with acetone and resuspended with an equal volume of 2× non-reducing SDS-PAGE sample buffer. Samples (10 µg total protein) were resolved by SDS-PAGE on 10% Tris-HCl resolving gels, electroblotted to Immobilon P polyvinylidene difluoride (PVDF) membrane and stored at -20°C for later use. To detect biotin-HPDP-labelled HSA Cys34, membranes were blocked for 1 h in 5% (w/v) non-fat dry milk in PBST [10 mM Na-phosphate, pH 7.2, 0.9% (w/v) NaCl, 0.1% (v/v) Tween 20] and probed with horseradish peroxidase (HRP)-conjugated streptavidin (1:5000 dilution) for 2 h in 5% (w/v)

non-fat dry milk in PBST. After washing in PBST, immunoreactive bands were detected by using enhanced chemiluminescence. Protein bands were then visualized by washing the membrane extensively in PBS and staining with Amido black.

### *2.9 Spectrophotometric determination of HSA carbonylation*

Protein carbonyl groups were quantified by adding an equal volume of 10 mM DNPH in 2 M HCl to the different HSA solutions (i.e., non-oxidized [control] HSA and HOCl-oxidized HSA samples). After 1-h incubation in the dark at room temperature, with gentle vortexing every 10 min, samples were precipitated with TCA (20% final concentration) and centrifuged at 13,000g in a tabletop microcentrifuge for 5 min, at room temperature. The supernatants were discarded and HSA pellets were washed once with 20% TCA and at least three times with 1 ml of ethanol/ethylacetate (1:1) to remove any free DNPH. Pellets were finally resuspended in 1 ml of 6 M guanidine hydrochloride (dissolved in 20 mM phosphate buffer, pH 2.3) at 37°C, for 15 min, with vortex mixing. Carbonyl contents were determined from the absorbance at 366 nm using a molar absorption coefficient of 22,000 M<sup>-1</sup> cm<sup>-1</sup> [28].

### *2.10 Determination of HSA carbonylation by Western blot analysis*

Carbonyl groups formed in HOCl-oxidized HSA samples and related control were determined by Western immunoblotting [29-31] after SDS-PAGE separation on 10% (w/v) Tris-HCl polyacrylamide gels of 10 µg total HSA samples and electroblotting to Immobilon P membrane. PVDF membranes were incubated for 5 min in 2 M HCl and for 5 min in DNPH (0.1 mg/ml in 2 M HCl). Subsequently, membranes were washed three times in 2 M HCl and seven times in 100% methanol, 5 min each, followed by one wash in PBST. After blocking the membranes with 5% (wt/vol) non-fat dry milk in PBST for 1 h, carbonyl formation was probed by a 2-h incubation with anti-DNP antibody (1:20,000 dilution) in 5% non-fat dry milk/PBST. After three washes with PBST for 5 min each, membranes were incubated with a 1:60,000 dilution of the HRP-linked secondary antibody in 5% non-fat dry milk/PBST for 1 h. After washing 3 times with PBST for 5 min each, immunostained HSA bands were visualized with enhanced chemiluminescence (ECL). In order to check equal protein loading among different lanes, membranes were finally stained with Amido Black.

### *2.11 Determination of dityrosine*

Dityrosine formation in oxidized samples of HSA, fibrinogen or a mixture of both was evaluated by analytical gel filtration high performance (pressure) liquid chromatography (HPLC) on a BioSep-SEC-S4000 column (300 mm × 7.8 mm) with a guard column (SecurityGuard™ GFC-4000, 4 mm length × 3 mm ID) and UV-VIS detector. Samples were prepared in 50 mM PBS, pH 7.4, at a final concentration of 1 mg/ml. 20 µg was loaded into the column for each sample. The mobile phase consisted of Milli-Q water, containing 0.5% (w/v) SDS and was eluted at 1 ml/min. Eluates were monitored both at 215 nm for measuring absorbance and at 415-nm emission with 325-nm excitation for measuring dityrosine fluorescence [32].

Dityrosine formation in plasma from hemodialyzed patients (n = 35, age range: 45-80) and age-matched healthy control subjects (n = 15) was evaluated by analytical gel filtration HPLC as described above. Plasma samples were diluted 1:15 in 50 mM Tris-HCl, pH 7.4 and 20 µl was loaded into the column for each sample. Eluates were monitored both at 215 nm for measuring protein absorbance and at 415-nm emission with 325-nm excitation for measuring dityrosine fluorescence. In the time range between 6 and 9 min, both the area under the 215-nm absorbance chromatogram and the area under the 415-nm emission fluorescence chromatogram were considered. The ratio between total fluorescence and total absorbance was calculated for each sample.

### *2.12 Determination of pentosidine*

Pentosidine formation in oxidized samples of HSA, fibrinogen or a mixture of both was evaluated by analytical gel filtration HPLC on a BioSep-SEC-S4000 column (300 mm × 7.8 mm) with a guard column (SecurityGuard™ GFC-4000, 4 mm length × 3 mm ID) and UV-VIS detector. Samples were prepared in 50 mM PBS, pH 7.4, at a final concentration of 1 mg/ml. 20 µg was loaded into the column for each sample. The mobile phase consisted of Milli-Q water, containing 0.5% (w/v) SDS and was eluted at 1 ml/min. Eluates were monitored both at 215 nm for measuring absorbance and at 385-nm emission with 335-nm excitation for measuring pentosidine fluorescence [33].

### *2.13 AOPP separation by SDS-PAGE*

AOPPs were separated by SDS-PAGE using 7.5% (w/v) polyacrylamide gels. Protein samples were added to an equal volume of 2× SDS-PAGE sample buffer [60 mM Tris-HCl, pH 6.8, 10% (v/v) glycerol, 2% (w/v) SDS, 0.01% (w/v) bromophenol blue, with (reducing conditions) or without (non-reducing conditions) 5% (w/v) DTT]. Samples were then heated at 95°C for 5 min



before being cooled and loaded onto the gel. Bands were visualized using Coomassie Brilliant Blue staining. Densitometric analysis of the gels was performed using Image J 1.40d software (National Institutes of Health, Bethesda, MD, USA).

#### 2.14 Protein identification by matrix-assisted laser desorption/ionization-time of flight (MALDI-TOF) mass spectrometry (MS) analysis

Protein bands were manually excised from silver-stained gels and processed as described in our previous paper [31]. One-microliter aliquots of the trypsin-digested protein supernatant were used for MS analysis on a Autoflex MALDI-TOF (Bruker) mass spectrometer. Spectra were accumulated for over a mass range of 700–4000 Da. Alkylation of cysteine by carbamidomethylation and oxidation of methionine were considered as fixed and variable modifications, respectively. One missed cleavage per peptide was allowed, and a mass tolerance of 0.5 Da was used in all searches. Peptides with masses correspondent to those of trypsin and matrix were excluded from the peak list. Proteins were identified by searching against a comprehensive non-redundant protein database (SwissProt 2014 08) using MASCOT programs via the internet [31].

### **3. Results**

#### *3.1 HOCl-induced oxidation of HSA*

HSA is a single polypeptide of 585 amino acids (66.5-kDa), including 18 tyrosine residues and 35 cysteine residues forming 17 intramolecular disulphide bonds, with the only free sulfhydryl group located at Cys34 [34]. When HSA samples (1 mg/ml, i.e. 15  $\mu$ M) were incubated with increasing concentrations of HOCl (ranging from 15 to 1500  $\mu$ M), the number of sulfhydryl groups, as determined by reaction with DTNB, drastically decreased from about 0.9 mol -SH/mol HSA to almost 0 mol -SH/mol HSA (Fig. 1A). Cys34 thiol oxidation was further established in a complementary experiment by using a biotin-based tagging technique, which have been applied with success to monitor the oxidation of protein -SH by reactive oxygen species [35,36]. The biotin tag can be detected at a level of sensitivity in the picomole range using immunoblotting with HRP-conjugated streptavidin. The loss of the biotin signal is proportional to the degree of thiol modification. Drastic oxidation of HSA Cys34 free sulfhydryl group by HOCl was confirmed by biotin-HPDP binding and Western blot analysis (Fig. 1B).

The extent of carbonyl-group formation in HSA exposed to HOCl, quantified by using the spectrophotometric DNPH assay, is shown in Fig. 1C. Increasing HOCl concentrations induced a progressive increase in HSA carbonylation, which was also determined by SDS-PAGE followed by immunoblotting using specific anti-DNP antibodies (Fig. 1D). Furthermore, levels of the cross-linked product dityrosine (di-Tyr) were increased, as assessed by fluorescence (Fig. 43D), only up to 2.5-fold at the highest HOCl concentration (i.e., 1500  $\mu$ M).

### *3.2 HOCl-induced high molecular weight protein aggregates, under reducing and non-reducing conditions, in HSA, fibrinogen or HSA/fibrinogen solutions*

Fibrinogen is a 340 kDa plasma glycoprotein and the precursor to fibrin, which is the primary structural component of blood clots. Fibrinogen is composed of three pairs of different polypeptide chains termed A $\alpha$  (66 kDa), B $\beta$  (54 kDa) and  $\gamma$  (48 kDa). These chains are connected by 29 disulphide bonds, forming a dimeric molecule (A $\alpha$  B $\beta$   $\gamma$ )<sub>2</sub>, with no free sulfhydryl groups [37]. Fig. 32A shows a representative sample of isolated fibrinogen, prepared as described in Materials and Methods and HSA, separated by SDS-PAGE under reducing and non-reducing conditions and stained for total protein with Coomassie blue. We also performed some preliminary experiments with commercial fibrinogen from human plasma (cod. F4883, Sigma-Aldrich), which is bound to a minor amount of plasma interfering compounds than our human plasma-derived fibrinogen preparations (Fig. 2A). We have identified such fibrinogen-associated molecules in our plasma-derived fibrinogen preparations using MALDI-TOF MS (Fig. 2C). According to SDS-PAGE patterns, they resulted to be similar in both fibrinogen preparations, although quantitatively different, i.e., about 7% and 13% of the total protein amount in commercial fibrinogen and our fibrinogen preparation, respectively, as determined by densitometry on SDS-PAGE gel lanes. However, following treatment with HOCl, commercial human fibrinogen gave results comparable to those we obtained with our fibrinogen solutions (see, as an example, Fig. 2B). All the successive experiments were then performed using fibrinogen purified from human plasma as described in Materials and Methods.

Samples of non-oxidized and HOCl-treated HSA (1 mg/ml), fibrinogen (1 mg/ml), and HSA/fibrinogen mixture (both proteins at 0.5 mg/ml) were separated on SDS-PAGE under non-reducing conditions. The exposure of HSA to increasing concentrations of HOCl up to 1500  $\mu$ M did not cause distinct changes in the HSA electrophoretic pattern after SDS-PAGE separation under non-reducing conditions, except for a moderate band disappearance and smear at the highest HOCl concentrations (Fig. 32B). Differently, a marked disappearance of the fibrinogen hexamer band occurred at HOCl concentrations equal or higher than 375  $\mu$ M (Fig. 32B), with an apparent,

concurrent formation of larger aggregates at the highest HOCl concentrations, in particular in HSA/fibrinogen mixture (Fig. 32B).

### 3.3 HOCl-induced formation of dityrosine in HSA, fibrinogen, and HSA/fibrinogen solutions

Size-exclusion HPLC with fluorometric detection under non-reducing conditions of HSA, fibrinogen, and HSA/fibrinogen mixture exposed to HOCl allowed us to separate HMW protein aggregates resulting from di-Tyr cross-linking (Fig. 43). HOCl induced a very little increase in dityrosine fluorescence emission of HSA samples (Fig. 43D). Differently, HOCl caused a concentration-dependent progressive increase in dityrosine fluorescence in fibrinogen (Fig. 43E) and HSA/fibrinogen samples (Fig. 43F), as highlighted in Fig. 43G, where data are presented as dityrosine fluorescence intensity normalized to the protein concentration, as determined by absorbance at 215 nm (Fig. 43A-C), in the time frame 6-9 min.

As further proof that dityrosine cross-linking is responsible for HMW-AOPP formation, HSA, fibrinogen, and HSA/fibrinogen solutions exposed to HOCl were denatured by heating at 95°C and separated by SDS-PAGE under reducing conditions (Fig. 32C). A progressive increase in HMW-AOPPs was clearly evident in fibrinogen and in HSA/fibrinogen samples exposed to HOCl concentrations higher than 150 µM, whereas no aggregate formation was observed in HSA samples. For the sake of clarity, we define HMW-AOPPs all protein aggregates with molecular weight (very) higher than 200 kDa under reducing conditions. Namely, those that formed a high molecular weight band at the beginning of the running gel (7.5% polyacrylamide) and very large aggregates that did not even enter the stacking gel (4% polyacrylamide) when the samples were run under reducing SDS-PAGE. This experiment demonstrated that HMW-AOPPs are extremely stable and resistant to reduction with DTT and thermal denaturation.

### 3.4 HOCl-induced formation of pentosidine in fibrinogen and HSA/fibrinogen solutions

In the plasma of chronic uremic patients AOPP levels also correlated with concentration of the advanced glycation end-product (AGE), pentosidine [8,11-13], a stable cross-link between arginine and lysine, which can be detected at very low concentrations based upon its fluorescence properties [33]. We analysed protein bound pentosidine in HSA, fibrinogen, and HSA/fibrinogen mixture exposed to HOCl by means of size-exclusion HPLC with fluorometric detection under non-reducing conditions (Fig. 54). A marked increase in pentosidine fluorescence was detected in fibrinogen and HSA/fibrinogen samples, whereas negligible pentosidine-related fluorescence was measured in HSA samples.

### 3.4 Contribution of fibrinogen in HOCl-induced formation of HMW-AOPPs

To confirm the key role played by fibrinogen in intermolecular dityrosine cross-linking and, probably, related formation of HMW-AOPPs, control and HOCl-exposed HSA/fibrinogen mixtures containing fibrinogen ranging from 0-100%, and, complementarily, HSA ranging from 100-0% were separated by reducing SDS-PAGE (Fig. 65). Protein samples exposed to 750  $\mu$ M HOCl exhibited a progressive increase in HMW-AOPP content with the increase in fibrinogen concentration (Fig. 65B), whereas control samples did not show any HMW-AOPP formation (Fig. 65A). Densitometric analysis of the Coomassie blue-stained gel highlighted the increase in HMW-AOPP formation with the increase in fibrinogen concentration in HSA/fibrinogen mixtures exposed to HOCl (not shown).

In a parallel experiment, control and HOCl-exposed HSA/fibrinogen mixtures containing 0-100% fibrinogen and, complementarily, 100-0% HSA were separated by size-exclusion HPLC with fluorometric detection under non-reducing conditions (Fig. 76). Protein samples exposed to HOCl clearly exhibited a progressive increase in di-Tyr fluorescence intensity with the increase in fibrinogen concentration (Fig. 76E). In Fig. 76E data are presented as dityrosine fluorescence intensity (Fig. 7D), normalized to protein concentration (as determined by absorbance at 215 nm, Fig. 76B) plotted against protein percentage composition by weight of HSA/fibrinogen mixtures exposed to 750  $\mu$ M HOCl. Differently, protein samples not exposed to HOCl exhibited negligible di-Tyr fluorescence (Fig. 76C). A positive correlation was obtained by plotting the di-Tyr fluorescence intensity normalized to protein concentration shown in Fig. 76E against the content of HMW-AOPPs in corresponding SDS-PAGE bands (as determined by densitometry of Coomassie blue-stained gels) (not shown), indicating that fibrinogen-dependent di-Tyr intermolecular cross-linking is the major contributor to HMW-AOPP formation in HOCl-exposed HSA/fibrinogen mixtures.

### 3.5 Contribution of fibrinogen in HOCl-induced formation of HMW-AOPPs in human plasma

The contribution of fibrinogen to AOPP formation was also evaluated in human plasma. For this purpose, we prepared different types of plasma: fibrinogen-free plasma, reconstituted plasma, i.e., defibrinogenized plasma added with fibrinogen at physiological concentration, and fibrinogen-enriched plasma, i.e., defibrinogenized plasma added with fibrinogen at a concentration five-fold greater than the physiological one. Control and HOCl-treated human plasma samples, conveniently diluted, were separated by size-exclusion HPLC with fluorometric detection under non-reducing

conditions (Fig. 87). Chromatograms obtained from HOCl-treated plasma samples showed that fibrinogen is the main contributor to di-Tyr fluorescence in normal (Fig. 87E) and reconstituted (Fig. 87G) plasma and that di-Tyr fluorescence is decreased in defibrinogenized plasma (Fig. 87F) compared with normal and reconstituted plasma, whereas it is considerably increased in fibrinogen-enriched plasma (Fig. 87H) compared with normal and reconstituted plasma.

#### 4. Discussion

In the present study, we found that exposure of HSA to HOCl concentrations  $\geq 75 \mu\text{M}$  causes oxidation of more than 90% of its Cys34 thiol (Fig. 1A and B), increasing protein carbonylation (Fig. 1C and D), poor dityrosine formation due to intramolecular cross-linking (Fig. 43D), no dityrosine formation due to intermolecular cross-linking as assessed by reducing SDS-PAGE (Fig. 32C) and no pentosidine formation (Fig. 54). These observations are in agreement with previous studies performed on HOCl-modified albumin [39] or plasma proteins of uremic patients [40,41].

Differently, incubation of fibrinogen or HSA/fibrinogen mixture with HOCl at concentrations higher than  $150 \mu\text{M}$  induced the formation of high molecular weight ( $>200 \text{ kDa}$ ) aggregates, some of which hardly entered the 7.5% polyacrylamide resolving gel and others did not even enter the stacking gel (4% polyacrylamide) (Fig. 32B and C). The concentrations of HOCl *in vivo* are estimated to be  $12\text{--}250 \mu\text{M}$  [42]; in particular, HOCl levels in the vicinity of activated neutrophils are at or above  $100 \mu\text{M}$  [43], being estimated to reach as high as  $5 \text{ mM}$  [44]. As the fibrinogen molecule has no free sulfhydryl groups, whereas it contains 134 tyrosine residues [45], such fibrinogen or HSA/fibrinogen aggregates could be mainly due to dityrosine cross-linking, as also suggested by the presence of such high molecular weight aggregates also when the samples exposed to HOCl concentrations  $\geq 375 \mu\text{M}$  were run under reducing SDS-PAGE (Fig. 32C). Formation of dityrosine in fibrinogen and HSA/fibrinogen samples exposed to HOCl was confirmed by means of size-exclusion HPLC with fluorometric measurement of di-Tyr fluorescence (Fig. 43). Simultaneous disappearance of the three fibrinogen polypeptide chain bands in fibrinogen or HSA/fibrinogen samples exposed to HOCl concentrations higher than  $150 \mu\text{M}$  and electrophoresed under reducing conditions (Fig. 32C) suggests the presence of intermolecular dityrosine cross-links and also supports the concept that oxidized fibrinogen, instead of albumin, is the key protein for intermolecular dityrosine formation, which in turn could be key for HMW-AOPP formation. This hypothesis is backed by the positive correlation between the increase in dityrosine and high molecular weight aggregate formation and the increase in fibrinogen concentration in samples containing a mixture of HSA and fibrinogen, exposed to  $750 \mu\text{M}$  HOCl (Figs. 65 and 76). Fibrinogen susceptibility to intermolecular di-Tyr linkages *in vitro* is supported by previous studies

where the protein was exposed to peroxynitrite [46] or to metal ion-catalyzed oxidation [47]. In samples containing HOCl-exposed HSA/fibrinogen mixtures, the intensity of di-Tyr fluorescence increases almost linearly as the band intensity of HMW-AOPPs increases (not shown), suggesting a central role for intermolecular di-Tyr cross-linking of fibrinogen in HMW-AOPP formation. This conclusion is corroborated by experiments where di-Tyr fluorescence was measured in HOCl-treated plasma samples containing physiological or supra-physiological fibrinogen concentrations or selectively depleted of fibrinogen (Fig. 87), which highlighted that fibrinogen is responsible for the highest fluorescence from dityrosine (Fig. 87E, G and H), even though other plasma protein(s) too contribute to it (Fig. 87F). Our findings confirm and extend a previous study, which suggested from indirect evidence that oxidized fibrinogen is a key molecule responsible for AOPP formation in the blood of patients with various peripheral vascular and cardiovascular diseases and, as a consequence, fibrinogen would contribute to  $A_{340}$  under acidic conditions [21,22].

In summary, our study provides in vitro evidence that oxidized fibrinogen may play a key role in HMW-AOPP formation, although the involvement of other protein(s) in HMW-AOPP formation in human plasma cannot be excluded and warrants further investigation. It is also worth considering that plasma fibrinogen is a heterogeneous mixture of fibrinogen variants [48]. For instance, the oxidation status of plasma-derived fibrinogen may be variable related to inter-individual factors, which could influence interaction of fibrinogen variants with delipidized HSA used in our study. However, we always extracted fibrinogen from at least 12-15 plasma samples, which were pooled before extraction and, therefore, we think this reduces at least some inter-individual differences. Indeed, we performed each experiment at least three times, each time purifying a new solution of fibrinogen from pooled samples of human plasma, obtaining similar results. On the other hand, albumin isolated from blood serum or plasma is usually heterogeneous, mainly because of the variable extent of oxidation of the Cys-34 thiol group and variations in the number and types of bound fatty acids. In the present work, we have therefore used commercial delipidized HSA that we converted to fully reduced HSA, in which the single free thiol of Cys34 is completely reduced. Moreover, cross-link formation of HOCl-treated HSA independent of dityrosine formation was recently described in a study showing irreversible inhibition of the HDL receptor, scavenger receptor class B, type 1, promoted by covalent cross-linking of HOCl-oxidized HSA (i.e., the so-called AOPP-albumin) via *N*-chloramines formed within lysine residues [49]. Conversion of positively charged  $\epsilon$ -amino groups of lysine residues by HOCl results in loss of positive charge through formation of *N*-chloramines. In our samples, chloramine generation was likely mostly reversed by addition of free methionine to HOCl-treated samples to stop HOCl reactivity. However, the possibility that other types of covalent cross-links, besides dityrosine formation, may contribute to HMW-AOPP formation in human plasma cannot be excluded and warrants further investigation.

The development of validated biomarkers for human diseases is essential to improve diagnosis and accelerate the development of new therapies. The collection of small blood volumes is mostly unproblematic and non-invasive biomarkers deliver an advantage over more invasive biomarkers. Because of their ease of determination, by taking advantage of their absorbance at 340 nm under acidic conditions, and stability (AOPPs remained stable during sample storage both at -20°C and -80°C for about six months [38]), increased plasma level of AOPPs is used as an economic indicator of oxidative stress in many diseases, amongst which chronic kidney disease [11,50], inflammatory bowel disease [51], coronary artery disease [9], idiopathic Parkinson's disease [52], and metabolic syndrome [53]. Unfortunately, hemolysis, blood-sampling under non-fasting conditions, high triglycerides, and freeze/thaw cycles can markedly interfere with AOPP measurement, mainly because of sample turbidity following lipid precipitation in plasma samples [11,20]. An additional step that includes precipitation of triglycerides and esterified cholesterol in the form of VLDL and LDL reduces, but does not solve, the turbidity problem [54]. A further improved method that uses citric acid to solubilize plasma lipids before absorbance measurement seems to detect AOPPs with better reproducibility and accuracy compared to previously reported methods [55].

Another problem, strictly related to poor reproducibility and accuracy of most current colorimetric methods for AOPP detection, is the lack of reliable, validated AOPP reference values in healthy humans: reported AOPP concentrations in healthy humans range from  $29.4 \pm 4.9 \mu\text{M}$  to  $170.9 \pm 101.9 \mu\text{M}$  [22]. The recently developed method that uses citric acid as the solvent [55] should allow a more accurate measure of chromophore absorption at 340 nm and, therefore, could help determine reliable AOPP reference values in healthy subjects. However, measuring AOPPs in diluted plasma as absorbance at 340 nm is a rather non-selective way to determine the level of oxidized proteins. It is thus necessary to take precautions to minimize the contribution of species other than AOPPs. In this respect, determination of dityrosine in AOPPs by HPLC with fluorometric detection could be used, in addition to the above-mentioned method, for further studies in order to clarify the role of AOPPs in human disease. To this end, preliminary results from analysis of plasma samples taken from uraemic patients undergoing hemodialysis by size-exclusion HPLC with fluorometric detection show a marked ( $p < 0.001$ ) increase in dityrosine fluorescence (normalized to protein concentration) as compared to healthy controls (Fig. 98).

### **Conflict of interest statement**

The authors declare no conflicts of interest.

## Acknowledgments

This research was supported by Fondazione Ariel ([www.fondazioneariel.it](http://www.fondazioneariel.it)), Rozzano (MI), Italy. The authors are grateful to Dr. Barbara Ponzini and all the personnel at the Analysis Laboratory, Department of Pathophysiology and Transplantation, University of Milan, for their invaluable support in providing blood samples from healthy subjects.

## References

- [1] Dalle-Donne I., Scaloni A., Giustarini D., Cavarra E., Tell G., Lungarella G., Colombo R., Rossi R., Milzani A. Proteins as biomarkers of oxidative/nitrosative stress in diseases: The contribution of redox proteomics. *Mass Spectrom. Rev.* 2005; **24**:55–99.
- [2] Dalle-Donne I., Rossi R., Colombo R., Giustarini D., Milzani A. Biomarkers of oxidative damage in human disease. *Clin. Chem.* 2006; **52**:601-623.
- [3] Bachi A., Dalle-Donne I., Scaloni A. Redox proteomics: Chemical principles, methodological approaches and biological/biomedical promises. *Chem. Rev.* 2013; **113**:596–698.
- [4] Levine R.L., Stadtman E.R. Oxidative modification of proteins during aging. *Exp. Gerontol.* 2001; **36**:1495–1502.
- [5] Rossi R., Giustarini D., Milzani A., Dalle-Donne I. Cysteinylation and homocysteinylation of plasma protein thiols during ageing of healthy human beings. *J. Cell. Mol. Med.* 2009; **13**:3131-3140.
- [6] Dalle-Donne I., Aldini G., Carini M., Colombo R., Rossi R., Milzani A. Protein carbonylation, cellular dysfunction, and disease progression. *J. Cell. Mol. Med.* 2006; **10**:389-406.
- [7] Baraibar M.A., Liu L., Ahmed E.K., Friguet B. Protein oxidative damage at the crossroads of cellular senescence, aging, and age-related diseases. *Oxid. Med. Cell Longev.* 2012; **2012**:919832.
- [8] Witko-Sarsat V., Friedlander M., Capeillere-Blandin C., Nguyen-Khoa T., Nguyen A.T., Zingraff J., Jungers P., Descamps-Latscha B. Advanced oxidation protein products as a novel marker of oxidative stress in uremia. *Kidney Int.* 1996; **49**:1304–1313.
- [9] Barsotti A., Fabbi P., Fedele M., Garibaldi S., Balbi M., Bezante G.P., Risso D., Indiveri F., Ghigliotti G., Brunelli C. Role of advanced oxidation protein products and thiol ratio in patients with acute coronary syndromes. *Clin. Biochem.* 2011; **44**:605-611.
- [10] Colombo G., Clerici M., Giustarini D., Gagliano N., Rossi R., Milzani A., Dalle-Donne I. Redox albuminomics: oxidized albumin in human diseases. *Antioxid. Redox Signal.* 2012; **17**:1515-1527.



- [11] Capeillère-Blandin C., Gausson V., Descamps-Latscha B., Witko-Sarsat V. Biochemical and spectrophotometric significance of advanced oxidized protein products. *Biochim. Biophys. Acta* 2004; **1689**:91–102.
- [12] Capeillère-Blandin C., Gausson V., Nguyen A.T., Descamps-Latscha B., Drueke T., Witko-Sarsat V. Respective role of uremic toxins and myeloperoxidase in the uremic state. *Nephrol. Dial. Transplant.* 2006; **21**:1555–1563.
- [13] Marsche G., Frank S., Hrzencak A., Holzer M., Dirnberger S., Wadsack C., Scharnagl H., Stojakovic T., Heinemann A., Oetl K. Plasma-Advanced Oxidation Protein Products are potent high-density lipoprotein receptor antagonists in vivo. *Circ. Res.* 2009; **104**:750-757.
- [14] Witko-Sarsat V., Gausson V., Nguyen A.T., Touam M., Drueke T., Santangelo F., Descamps-Latscha B. AOPP-induced activation of human neutrophil and monocyte oxidative metabolism: a potential target for N-acetylcysteine treatment in dialysis patients. *Kidney Int.* 2003; **64**:82–91.
- [15] Guo Z.J., Niu H.X., Hou F.F., Zhang L., Fu N., Nagai R., Lu X., Chen B.H., Shan Y.X., Tian J.W., Nagaraj R.H., Xie D., Zhang X. Advanced oxidation protein products activate vascular endothelial cells via a RAGE-mediated signaling pathway. *Antioxid. Redox Signal.* 2008; **10**:1699–1712.
- [16] Shi X.Y., Hou F.F., Niu H.X., Wang G.B., Xie D., Guo Z.J., Zhou Z.M., Yang F., Tian J.W., Zhang X. Advanced oxidation protein products promote inflammation in diabetic kidney through activation of renal nicotinamide adenine dinucleotide phosphate oxidase. *Endocrinology* 2008; **149**:1829–1839.
- [17] Liu S.X., Hou F.F., Guo Z.J., Nagai R., Zhang W.R., Liu Z.Q., Zhou Z.M., Zhou M., Xie D., Wang G.B., Zhang X. Advanced oxidation protein products accelerate atherosclerosis through promoting oxidative stress and inflammation. *Arterioscler. Thromb. Vasc. Biol.* 2006; **26**:1156–1162.
- [18] Cao W., Xu J., Zhou Z.M, Wang G.B., Hou F.F., Nie J. Advanced Oxidation Protein Products activate intrarenal renin–angiotensin system via a CD36-mediated, redox-dependent pathway. *Antioxid. Redox Signal.* 2013; **18**:19–35.
- [19] Rodriguez-Ayala E., Anderstam B., Suliman M.E., Seeberger A., Heimbürger O., Lindholm B., Stenvinkel P. Enhanced RAGE-mediated NF- $\kappa$ B stimulation in inflamed hemodialysis patients. *Atherosclerosis* 2005; **180**:333–340.
- [20] Valli A., Suliman M.E., Meert N., Vanholder R., Lindholm B., Stenvinkel P., Watanabe M., Barany P., Alvestrand A., Anderstam B. Overestimation of advanced oxidation protein products in uremic plasma due to presence of triglycerides and other endogenous factors. *Clin. Chim. Acta* 2007; **379**:87–94.

- [21] Selmeçi L., Székely M., Soós P., Seres L., Klinga N., Geiger A., Acsády G. Human blood plasma advanced oxidation protein products (AOPP) correlates with fibrinogen levels. *Free Radic. Res.* 2006; **40**:952–958.
- [22] Selmeçi L. Advanced oxidation protein products (AOPP): novel uremic toxins, or components of the non-enzymatic antioxidant system of the plasma proteome? *Free Radic. Res.* 2011; **45**:1115–1123.
- [23] Chen Y.H., Shi W., Liang X.L., Liang Y.Z., Fu X. Effect of blood sample type on the measurement of advanced oxidation protein products as a biomarker of inflammation and oxidative stress in hemodialysis patients. *Biomarkers* 2011; **16**:129-135.
- [24] Paton L.N., Mocatta T.J., Richards A.M., Winterbourn C.C. Increased thrombin-induced polymerization of fibrinogen associated with high protein carbonyl levels in plasma from patients post myocardial infarction. *Free Radic. Biol. Med.* 2010; **48**:223-229.
- [25] Lowe G.D., Rumley A., Mackie I.J. Plasma fibrinogen. *Ann. Clin. Biochem.* 2004; **41**:430-440.
- [26] Ellman G.L. Tissue sulfhydryl groups. *Arch. Biochem. Biophys.* 1959; **82**:70–77.
- [27] Riddles P.W., Blakeley R.L., Zerner B. Reassessment of Ellman's reagent. *Methods Enzymol.* 1983; **91**:49–60.
- [28] Levine R.L., Williams J.A., Stadtman E.R., Shacter E. Carbonyl assays for determination of oxidatively modified proteins. *Methods Enzymol.* 1994; **233**:346–357.
- [29] Dalle-Donne I., Carini M., Vistoli G., Gamberoni L., Giustarini D., Colombo R., Maffei Facino R., Rossi R., Milzani A., Aldini G. Actin Cys374 as a nucleophilic target of alpha,beta-unsaturated aldehydes. *Free Radic. Biol. Med.* 2007; **42**:583–598.
- [30] Colombo G., Aldini G., Orioli M., Giustarini D., Gornati R., Rossi R., Colombo R., Carini M., Milzani A., Dalle-Donne I. Water-Soluble alpha,beta-unsaturated aldehydes of cigarette smoke induce carbonylation of human serum albumin. *Antioxid. Redox Signal.* 2010; **12**:349-364.
- [31] Colombo G., Dalle-Donne I., Orioli M., Giustarini D., Rossi R., Carini M., Aldini G., Milzani A., Butterfield D.A., Gagliano N. Oxidative damage in human gingival fibroblasts exposed to cigarette smoke. *Free Radic. Biol. Med.* 2012; **52**:1584-1596.
- [32] Dalle-Donne I., Rossi R., Giustarini D., Gagliano N., Lusini L., Milzani A., Di Simplicio P., Colombo R. Actin carbonylation: from a simple marker of protein oxidation to relevant signs of severe functional impairment. *Free Radic. Biol. Med.* 2001; **31**:1075–1083.
- [33] Sell DR, Monnier VM. Structure elucidation of a senescence cross-link from human extracellular matrix. Implication of pentoses in the aging process. *J. Biol. Chem.* 1989; **264**:21597-21602.

- [34] Carballal S., Alvarez B., Turell L., Botti H., Freeman B.A., Radi R. Sulfenic acid in human serum albumin. *Amino Acids* 2007; **32**:543-551.
- [35] Landar A., Oh J.Y., Giles N.M., Isom A., Kirk M., Barnes S., Darley-Usmar V.M. A sensitive method for the quantitative measurement of protein thiol modification in response to oxidative stress. *Free Radic. Biol. Med.* 2006; **40**:459-468.
- [36] Colombo G., Rossi R., Gagliano N., Portinaio N., Clerici M., Annibal A., Giustarini D., Colombo R., Milzani A., Dalle-Donne I. Red blood cells protect albumin from cigarette smoke-induced oxidation. *PLoS ONE* 2012; **7**:e29930.
- [37] Herrick S., Blanc-Brude O., Gray A., Laurent G. Fibrinogen. *Int. J. Biochem. Cell. Biol.* 1999; **31**:741-746.
- [38] Matteucci E., Biasci E., Giampietro O. Advanced oxidation protein products in plasma: stability during storage and correlations with other clinical characteristics. *Acta Diabetol.* 2001; **38**:187-189.
- [39] Fu S., Wang H., Davies M., Dean R. Reactions of hypochlorous acid with tyrosine and peptidyl-tyrosyl residues give dichlorinated and aldehydic products in addition to 3-chlorotyrosine. *J. Biol. Chem.* 2000; **75**:10851-10858.
- [40] Himmelfarb J., McMonagle E., McMenemy E. Plasma protein thiol oxidation and carbonyl formation in chronic renal failure. *Kidney Int.* 2000; **58**:2571-2578.
- [41] Himmelfarb J., McMonagle E. Albumin is the major plasma protein target of oxidant stress in uremia. *Kidney Int.* 2001; **60**:358-563.
- [42] McCall M.R., Carr A.C., Forte T.M., Frei B. LDL modified by hypochlorous acid is a potent inhibitor of lecithin-cholesterol acyltransferase activity. *Arterioscler. Thromb. Vasc. Biol.* 2001; **21**:1040-1045.
- [43] Foote, C.S., Goyne, T.E., Lehrer, R.I. Assessment of chlorination by human neutrophils. *Nature* 1983; **301**:715-716.
- [44] Weiss S.J. Tissue destruction by neutrophils. *N. Engl. J. Med.* 1989; **320**:365-376.
- [45] Mosesson M.W. Fibrinogen structure and fibrin clot assembly. *Semin. Thromb. Hemost.* 1998; **24**:169-174.
- [46] Nowak P., Zbikowska H.M., Ponczek M., Kolodziejczyk J., Wachowicz B. Different vulnerability of fibrinogen subunits to oxidative/nitrative modifications induced by peroxynitrite: functional consequences. *Thromb. Res.* 2007; **121**:163-174.
- [47] Tetik S., Kaya K., Demir M., Eksioglu-Demiralp E., Yardimci T. Oxidative modification of fibrinogen affects its binding activity to glycoprotein (GP) IIb/IIIa. *Clin. Appl. Thromb. Hemost.* 2010; **16**:51-59.

- [48] de Maat M.P., Verschuur M. Fibrinogen heterogeneity: inherited and noninherited. *Curr. Opin. Hematol.* 2005; **12**:377-383.
- [49] Binder V., Ljubojevic S., Haybaeck J., Holzer M., El-Gamal D., Schicho R., Pieske B., Heinemann A., Marsche G. The myeloperoxidase product hypochlorous acid generates irreversible high-density lipoprotein receptor inhibitors. *Arterioscler. Thromb. Vasc. Biol.* 2013; **33**:1020-1027.
- [50] Mayer B., Zitta S., Greilberger J., Holzer H., Reibnegger G., Hermetter A., Oetl K. Effect of hemodialysis on the antioxidative properties of serum. *Biochim. Biophys. Acta* 2003; **1638**:267–272.
- [51] Krzystek-Korpacka M., Neubauer K., Berdowska I., Boehm D., Zielinski B., Petryszyn P., Terlecki G., Paradowski L., Gamian A. Enhanced formation of advanced oxidation protein products in IBD. *Inflamm. Bowel Dis.* 2008; **14**:794-802.
- [52] García-Moreno J.M., Martín de Pablos A., García-Sánchez M.I., Méndez-Lucena C., Damas-Hermoso F., Rus M., Chacón J., Fernández E. May serum levels of advanced oxidized protein products serve as a prognostic marker of disease duration in patients with idiopathic Parkinson's disease? *Antioxid. Redox Signal.* 2013; **18**:1296-1302.
- [53] Korkmaz G.G., Altnoglu E., Civelek S., Sozer V., Erdenen F., Tabak O., Uzun H. The association of oxidative stress markers with conventional risk factors in the metabolic syndrome. *Metabolism* 2013; **62**:828-835.
- [54] Anderstam B., Bragfors-Helin A.C., Valli A., Stenvinkel P., Lindholm B., Suliman M.E. Modification of the oxidative stress biomarker AOPP assay: application in uremic samples. *Clin. Chim. Acta* 2008; **393**:114–118.
- [55] Hanasand M., Omdal R., Norheim K.B., Gøransson L.G., Brede C., Jonsson G. Improved detection of advanced oxidation protein products in plasma. *Clin. Chim. Acta* 2012; **413**:901-906.

## Figure legends

**Fig. 1.** HOCl-induced oxidation of HSA. (A,B) Effect of HOCl on HSA Cys34 sulfhydryl group as determined (A) by the Ellman assay and (B) by biotin-HPDP binding and Western blot analysis. (C,D) Effect of HOCl on HSA carbonylation. (C) Carbonyl formation was assessed from the absorbance at 366 nm after protein derivatization with DNPH. (D) The increase in HSA carbonyl

content was also analysed using reducing SDS-PAGE/Western blotting probed with anti-DNP antibodies. Data are presented as the mean  $\pm$  SD for three independent experiments. Immunoblots show representative images of three independent experiments.

**Fig. 2.** Electrophoretic patterns of commercial and our ammonium sulphate precipitated preparations of human fibrinogen. (A) Representative samples of commercial fibrinogen (CF) and our plasma-derived fibrinogen obtained by ammonium-sulphate precipitation (ASF) separated by SDS-PAGE (10% Tris-HCl resolving gels) under reducing conditions. The relative percentage of each polypeptide chain (P1, ... P12) to the total protein amount is indicated on the right. Molecular weight markers are indicated on the left. (B) Electrophoretic patterns (10% Tris-HCl resolving gels), under reducing conditions, of commercial and our ammonium sulphate precipitated preparations of human fibrinogen exposed to HOCl. (C) Identification, by MALDI-TOF MS analysis, of the main plasma interfering compounds present in our fibrinogen preparations. Protein bands were visualized by staining with Coomassie Blue G250. Representative gels of three independent experiments are shown.

**Fig. 32.** Electrophoretic patterns, under reducing and non-reducing conditions, of HSA, fibrinogen or HSA/fibrinogen mixtures containing 50% HSA and 50% fibrinogen by weight, exposed to HOCl. (A) Representative samples of isolated HSA and human fibrinogen prepared as described under Materials and Methods and separated by SDS-PAGE (10% Tris-HCl resolving gels) under reducing (with DTT) and non-reducing (without DTT) conditions; fibrinogen A $\alpha$  (66 kDa), B $\beta$  (54 kDa), and  $\gamma$  (48 kDa) chains are marked. Approximately 8  $\mu$ g of proteins were applied to each lane. (B) Samples of native and HOCl-treated HSA, fibrinogen and HSA/fibrinogen mixtures were separated by SDS-PAGE under non-reducing conditions. (C) Samples of native and HOCl-treated HSA, fibrinogen and HSA/fibrinogen mixtures were separated by SDS-PAGE under reducing conditions. In both (B) and (C), approximately 8  $\mu$ g of HSA or fibrinogen were applied to each lane, whereas approximately 16  $\mu$ g of HSA/fibrinogen mixtures were applied to each lane; the lane on the left shows high molecular weight protein markers. Protein bands were visualized by staining with Coomassie Blue R250. Representative gels of three independent experiments are shown.

**Fig. 43.** Determination of dityrosine in HSA, fibrinogen, and HSA/fibrinogen mixtures containing 50% HSA and 50% fibrinogen by weight, exposed to HOCl, by size-exclusion HPLC with fluorometric detection. HPLC profiles of (A and D) HSA, (B and E) fibrinogen, and (C and F) HSA/fibrinogen mixtures; protein samples were exposed to 15-1500  $\mu$ M HOCl but, for simplicity, only chromatograms relative to controls (solid line) and samples exposed to 375  $\mu$ M (dotted line) or

1500  $\mu\text{M}$  (dashed line) HOCl are shown. Eluates were monitored for absorbance at 215 nm to measure protein concentration (A-C) and for fluorescence with  $\lambda_{\text{ex}}$  at 325 nm and  $\lambda_{\text{em}}$  at 415 nm to measure di-Tyr fluorescence (D-F). In E and F, arrow indicates the di-Tyr fluorescence peak of HMW-AOPPs. Representative chromatograms of three independent experiments are shown. (G) Dityrosine fluorescence intensity at  $\lambda_{\text{em}} = 415$  nm (D-F) normalized to the protein concentration, as determined by absorbance at 215 nm (A-C) (calculated for the peak area in the time frame 6-9 min), was plotted versus HOCl concentrations for HSA (dotted line), fibrinogen (solid line), and HSA/fibrinogen mixtures (dashed line). Data are presented as the mean  $\pm$  SD for three independent measurements.

**Fig. 54.** Determination of pentosidine in HSA, fibrinogen, and HSA/fibrinogen mixtures containing 50% HSA and 50% fibrinogen by weight, exposed to HOCl, by size-exclusion HPLC with fluorometric detection. Eluates were monitored for absorbance at 215 nm to measure protein concentration and for fluorescence with  $\lambda_{\text{ex}}$  at 335 and  $\lambda_{\text{em}}$  at 385 nm to measure pentosidine fluorescence. Pentosidine fluorescence intensity normalized to the protein concentration (calculated for the peak area in the time frame 6-9 min) versus HOCl concentration is shown. Data are presented as the mean  $\pm$  SD for three independent measurements.

**Fig. 65.** Electrophoretic pattern, under reducing conditions, of HSA/fibrinogen mixtures, containing fibrinogen ranging from 0–100% and albumin ranging from 100–0%. (A) HSA/fibrinogen mixtures not exposed to HOCl. (B) HSA/fibrinogen mixtures exposed to 750  $\mu\text{M}$  HOCl. In both gels, approximately 8  $\mu\text{g}$  of proteins were applied to each lane. Protein bands were visualized by staining with Coomassie Blue R250. The lane on the left shows high molecular weight protein markers. Representative gels of three independent experiments are shown.

**Fig. 76.** Determination of dityrosine in HSA/fibrinogen mixtures containing fibrinogen ranging from 0–100% and albumin ranging from 100–0%, exposed to 750  $\mu\text{M}$  HOCl, by size-exclusion HPLC with fluorometric detection. (A and C) HSA/fibrinogen mixtures not exposed to HOCl. (B and D) HSA/fibrinogen mixtures exposed to 750  $\mu\text{M}$  HOCl. For simplicity, only chromatograms relative to samples containing 100% HSA/0% fibrinogen (solid line), 0% HSA/100% fibrinogen (dotted line) and 50% HSA/50% fibrinogen (dashed line) are shown. Eluates were monitored for absorbance at 215 nm to measure protein concentration (A and B) and for fluorescence with  $\lambda_{\text{ex}}$  at 325 nm and  $\lambda_{\text{em}}$  at 415 nm to measure di-Tyr fluorescence (C and D). In D, arrow indicates the di-Tyr fluorescence peak of HMW-AOPPs. Representative chromatograms of three independent experiments are shown. (E) Dityrosine fluorescence intensity at  $\lambda_{\text{em}} = 415$  nm of HOCl-treated

samples (D) normalized to the protein concentration, as determined by absorbance at 215 nm (B) (calculated for the peak area in the time frame 6-9 min), was plotted versus protein percentage composition by weight of HSA/fibrinogen mixtures exposed to 750  $\mu\text{M}$  HOCl. Data are presented as the mean  $\pm$  SD for three independent measurements.

**Fig. 87.** Determination of dityrosine in human plasma exposed to HOCl by size-exclusion HPLC with fluorometric detection. HPLC profiles of (A and E) human plasma, (B and F) fibrinogen-free plasma, (C and G) reconstituted plasma, i.e., defibrinogenized plasma added with fibrinogen at physiological concentration, and (D and H) fibrinogen-enriched plasma, i.e., defibrinogenized plasma added with fibrinogen at a concentration five-fold greater than the physiological one. Protein samples were exposed to 375  $\mu\text{M}$  (dotted line) or 1500  $\mu\text{M}$  HOCl (dashed line). Eluates were monitored for absorbance at 215 nm to measure protein concentration (A-D) and for fluorescence with  $\lambda_{\text{ex}}$  at 325 nm and  $\lambda_{\text{em}}$  at 415 nm to measure di-Tyr fluorescence (E-H). Representative chromatograms of three independent experiments are shown.

**Fig. 98.** Determination of dityrosine in human plasma from healthy subjects and hemodialyzed patients by size-exclusion HPLC with fluorometric detection. Eluates were monitored for absorbance at 215 nm to measure protein concentration and for fluorescence with  $\lambda_{\text{ex}}$  at 325 nm and  $\lambda_{\text{em}}$  at 415 nm to measure di-Tyr fluorescence. Significance between the two groups was determined by *t* test.

Figure 1

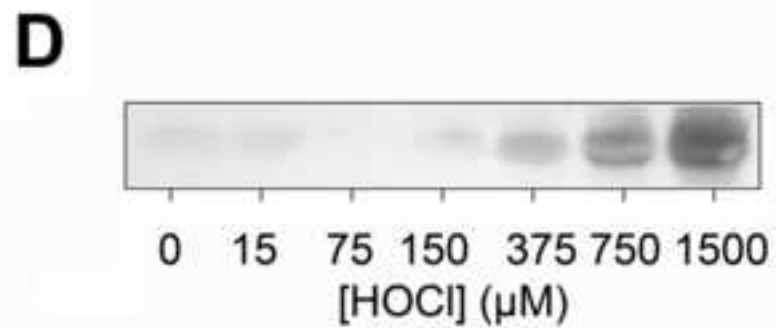
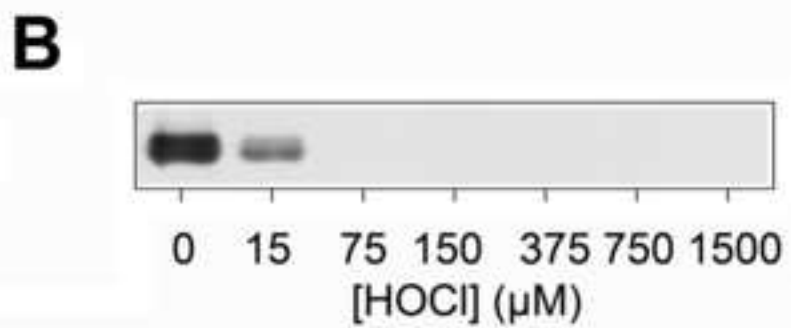
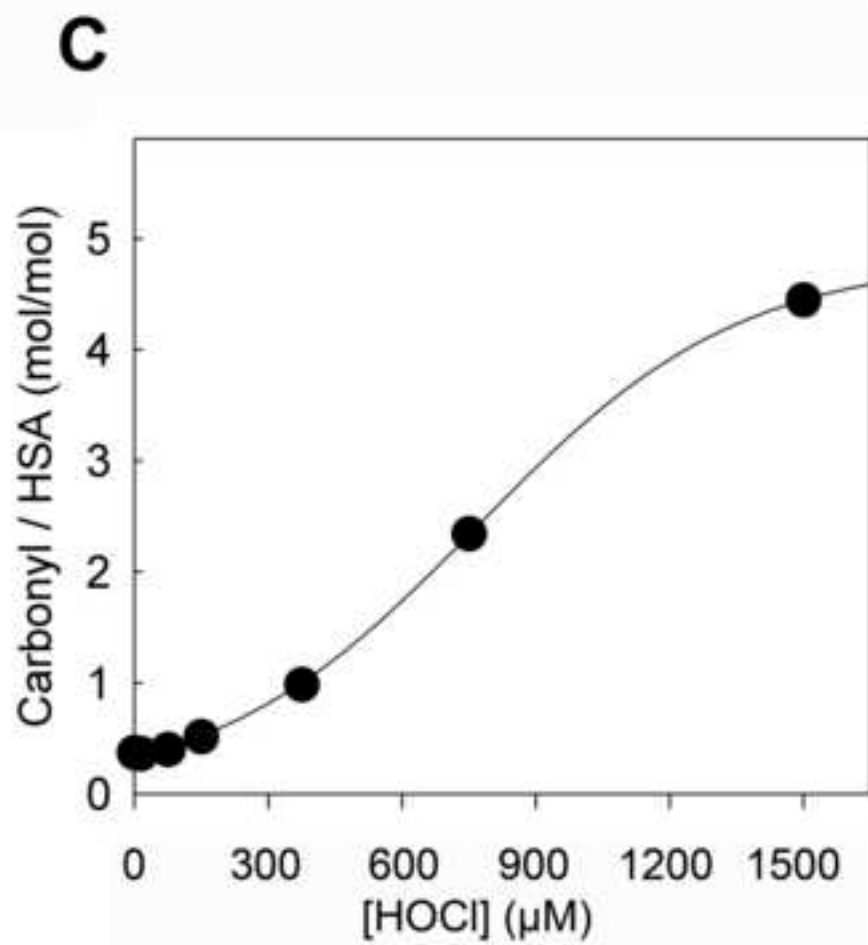
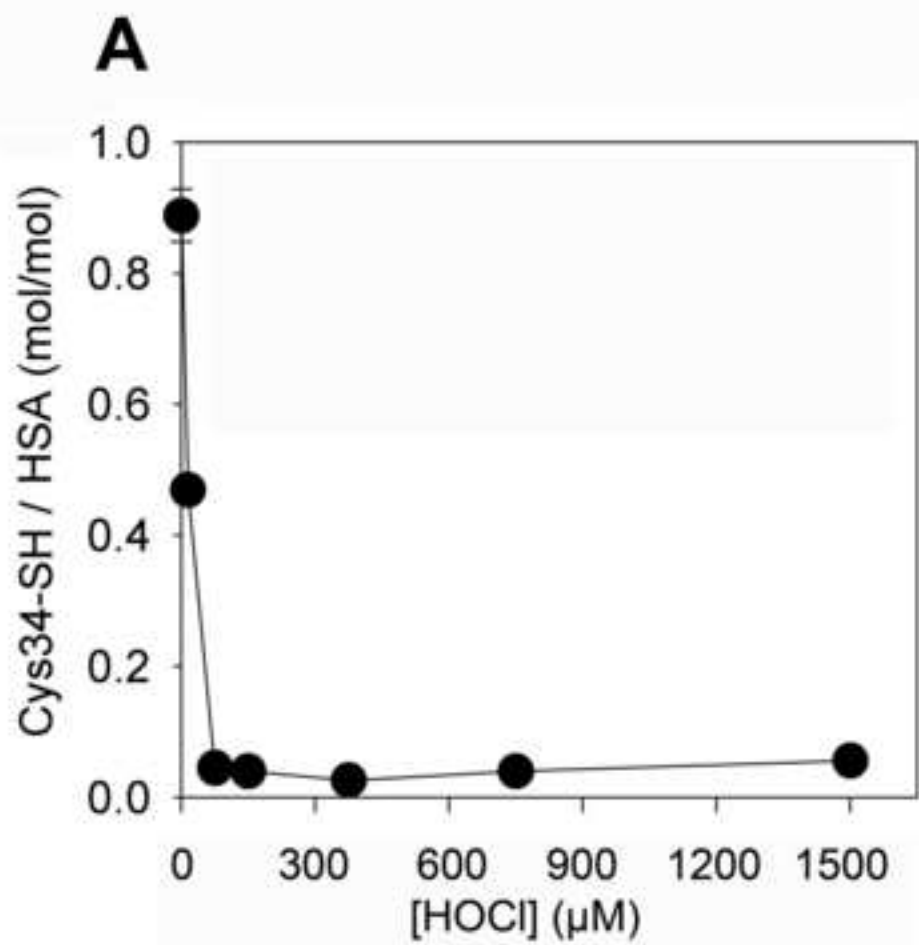




Figure 2

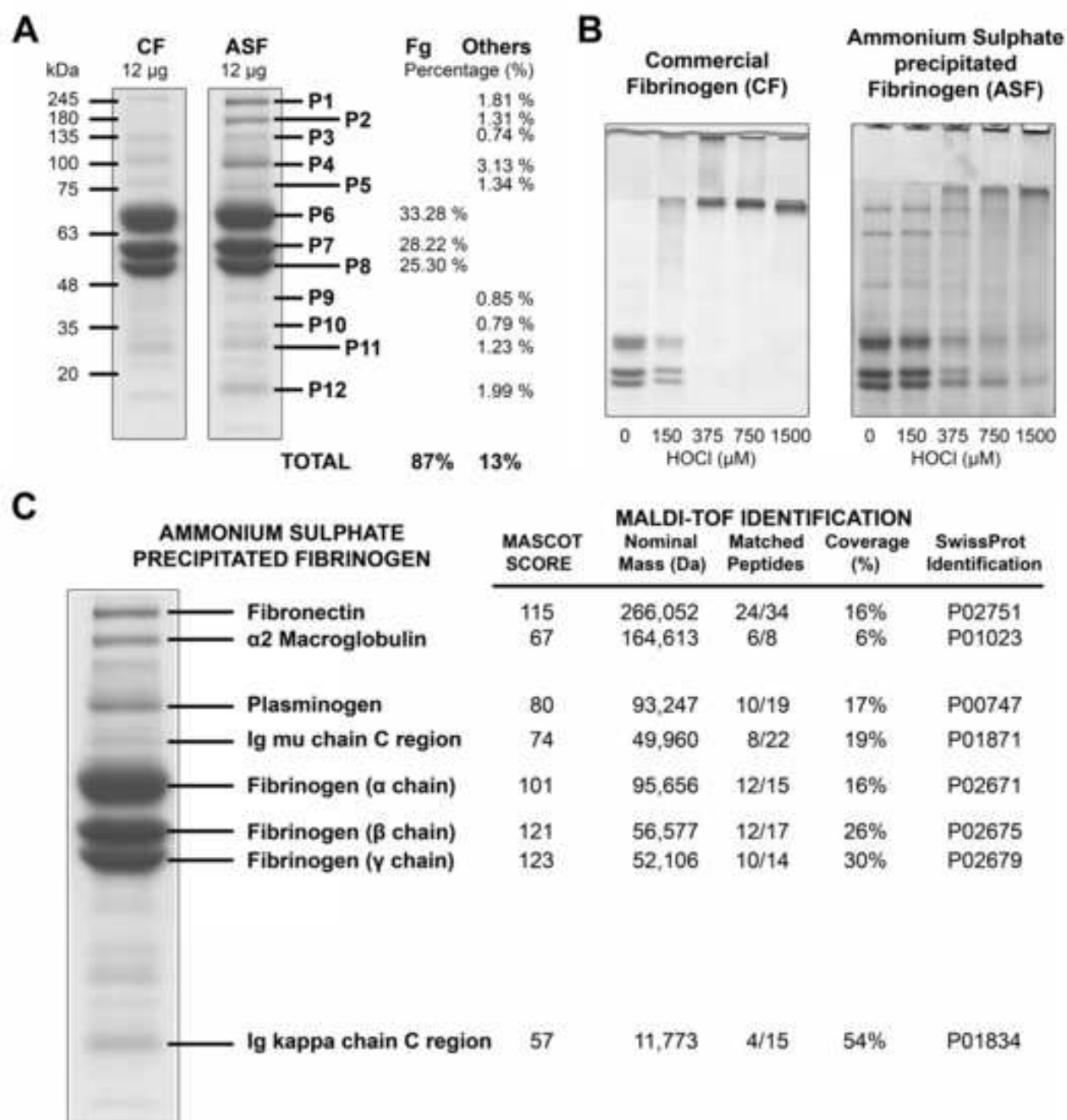
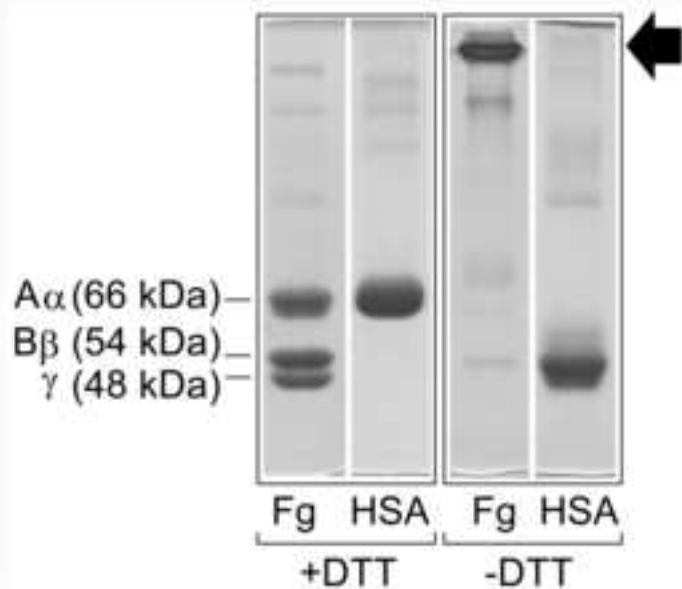
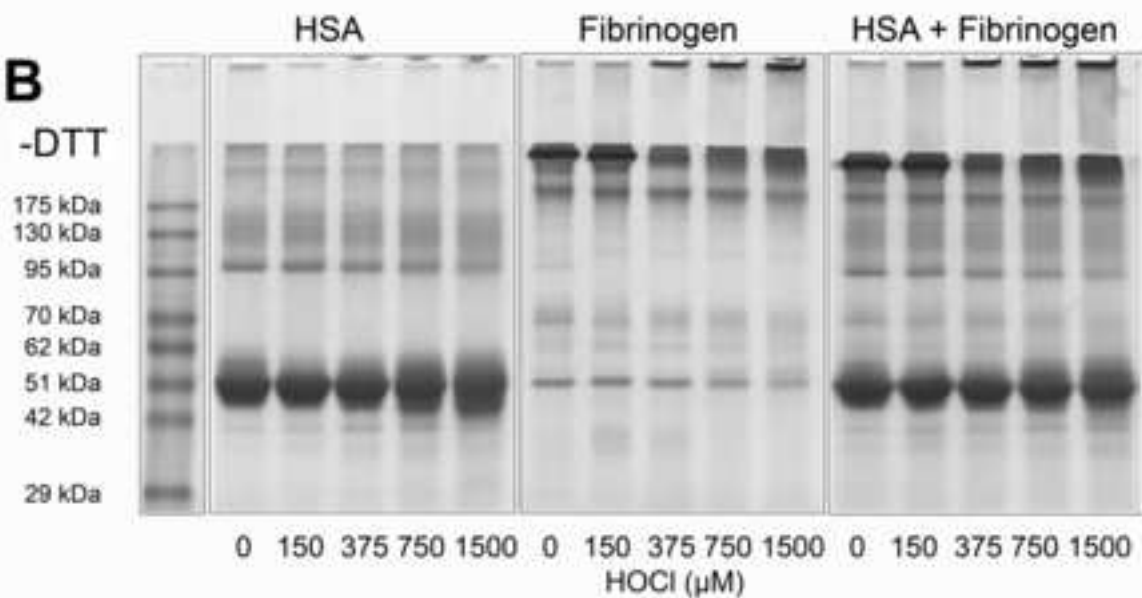


Figure 3

**A**



**B**



**C**

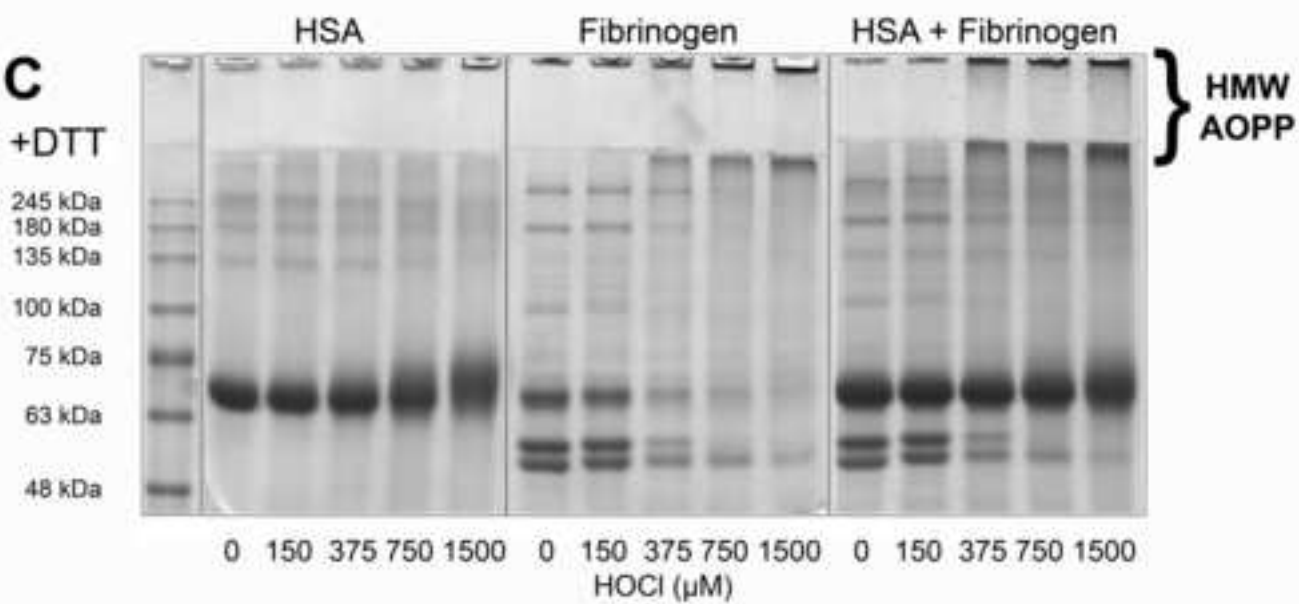


Figure 4

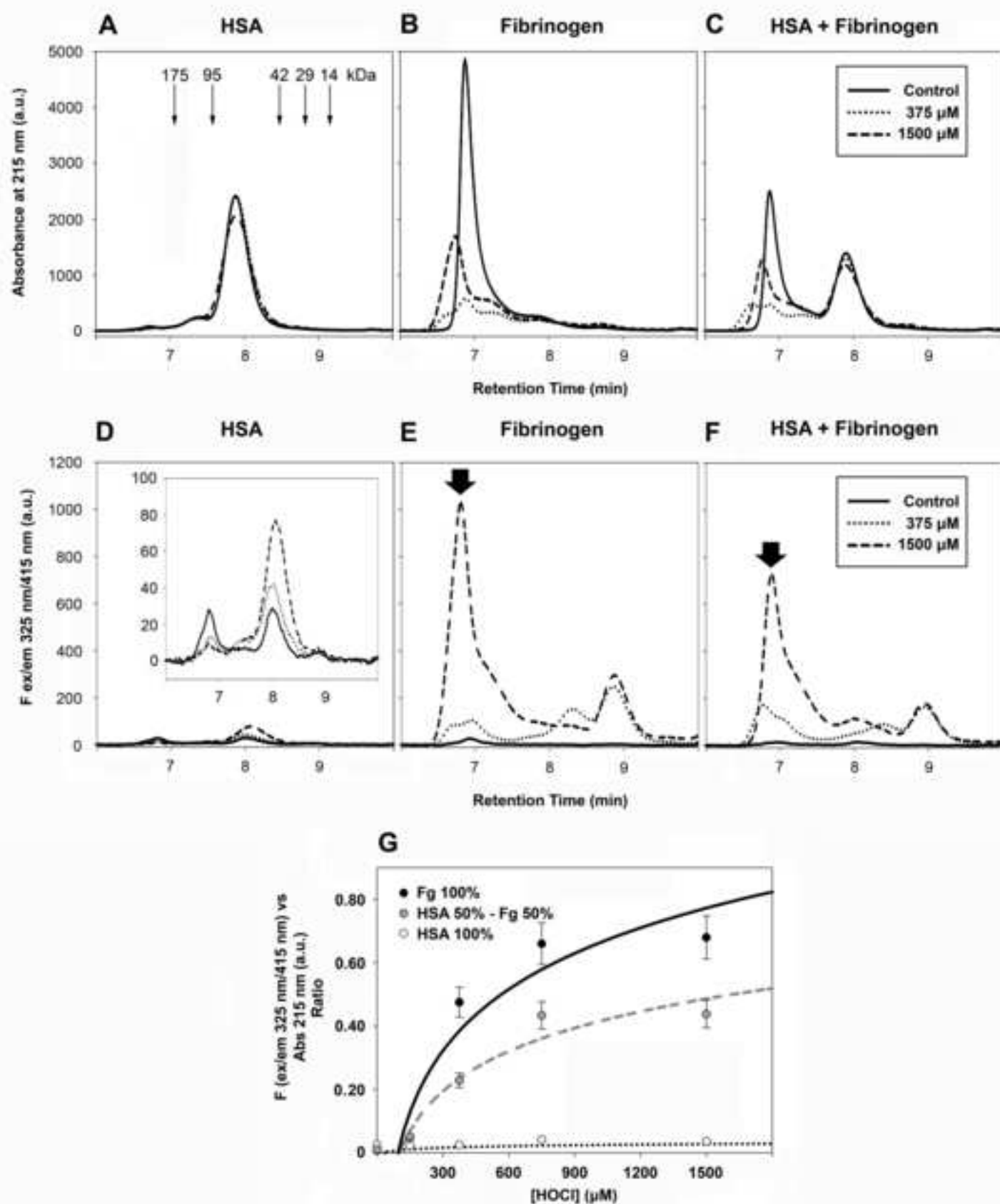


Figure 5

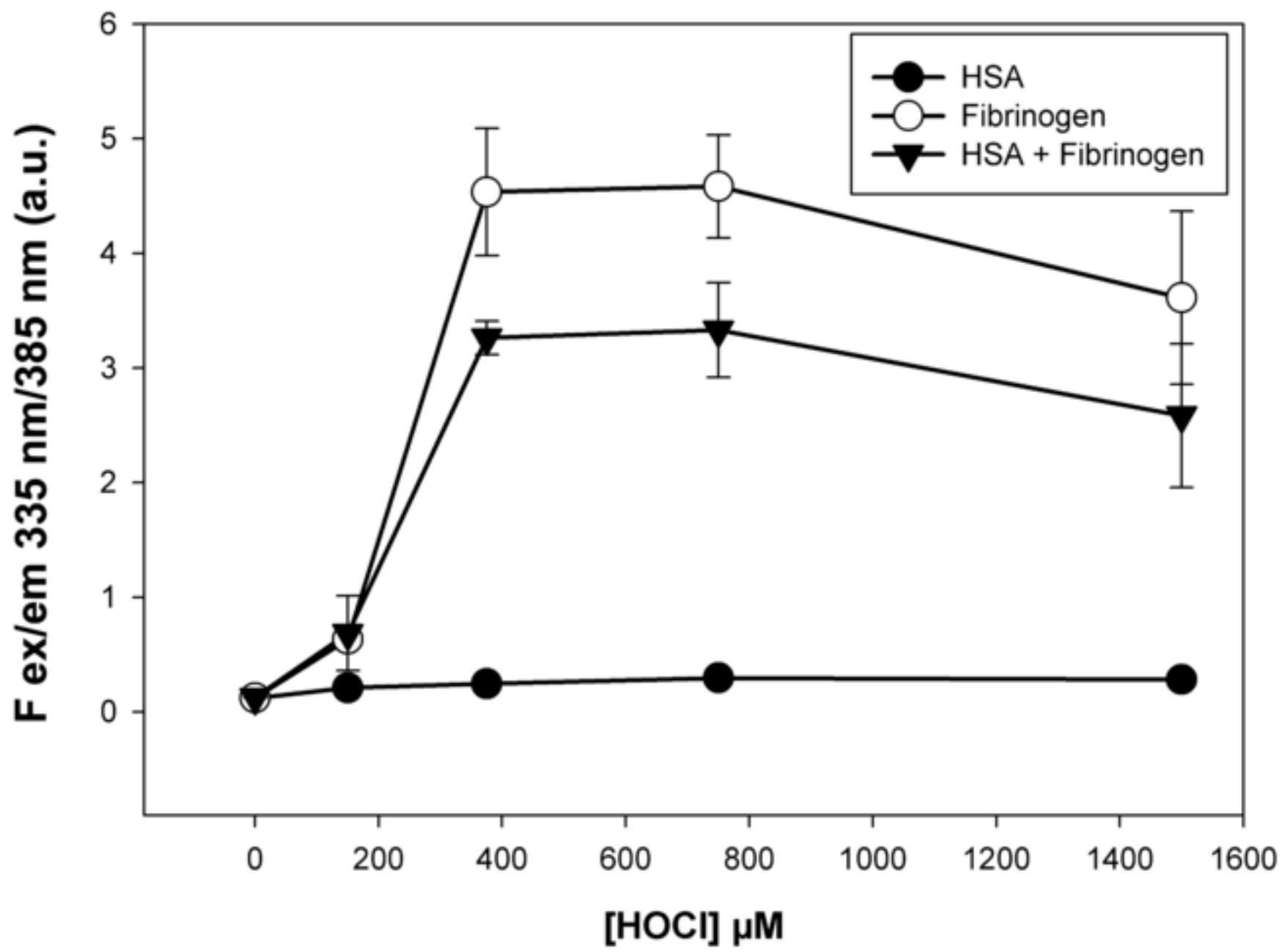
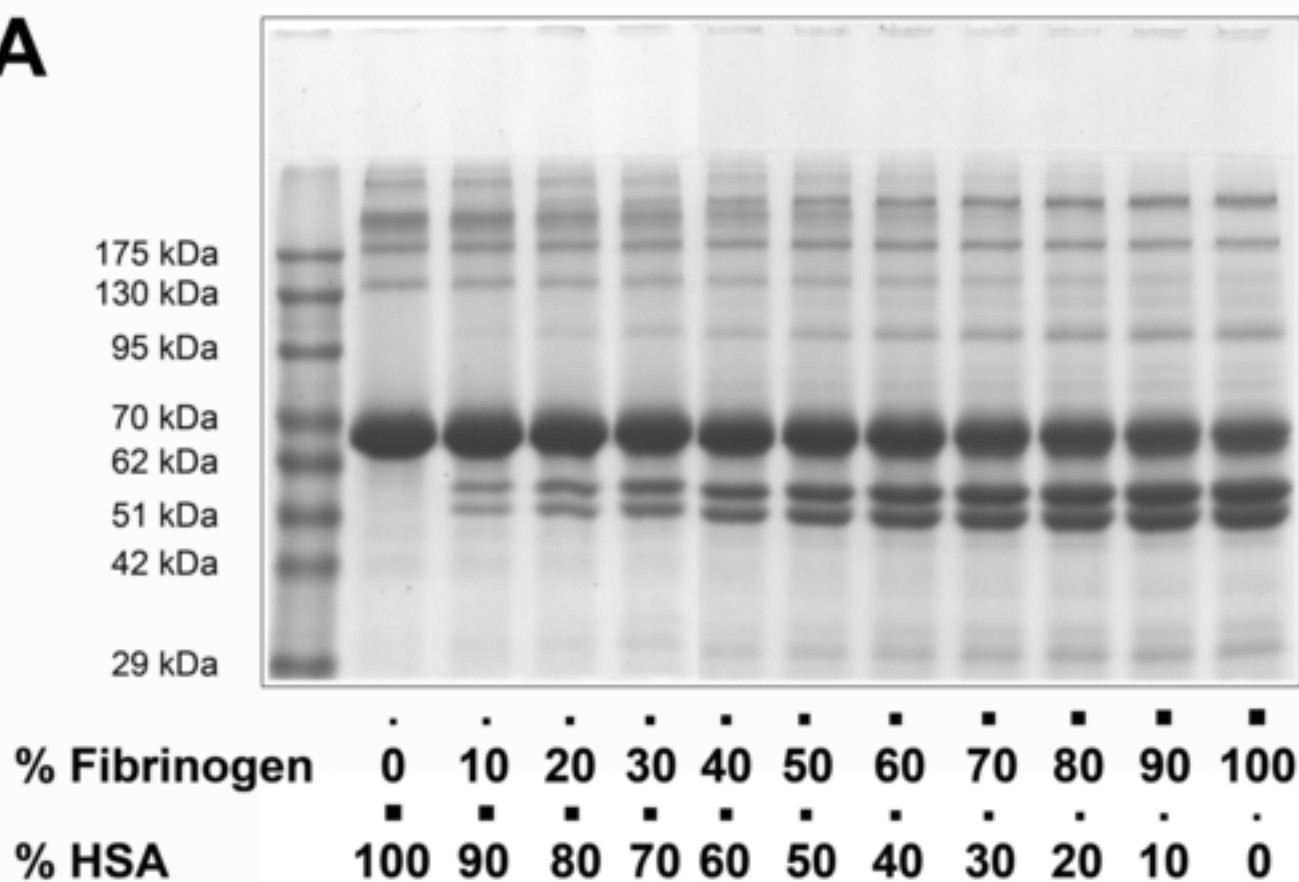


Figure 6

**A**



**B**

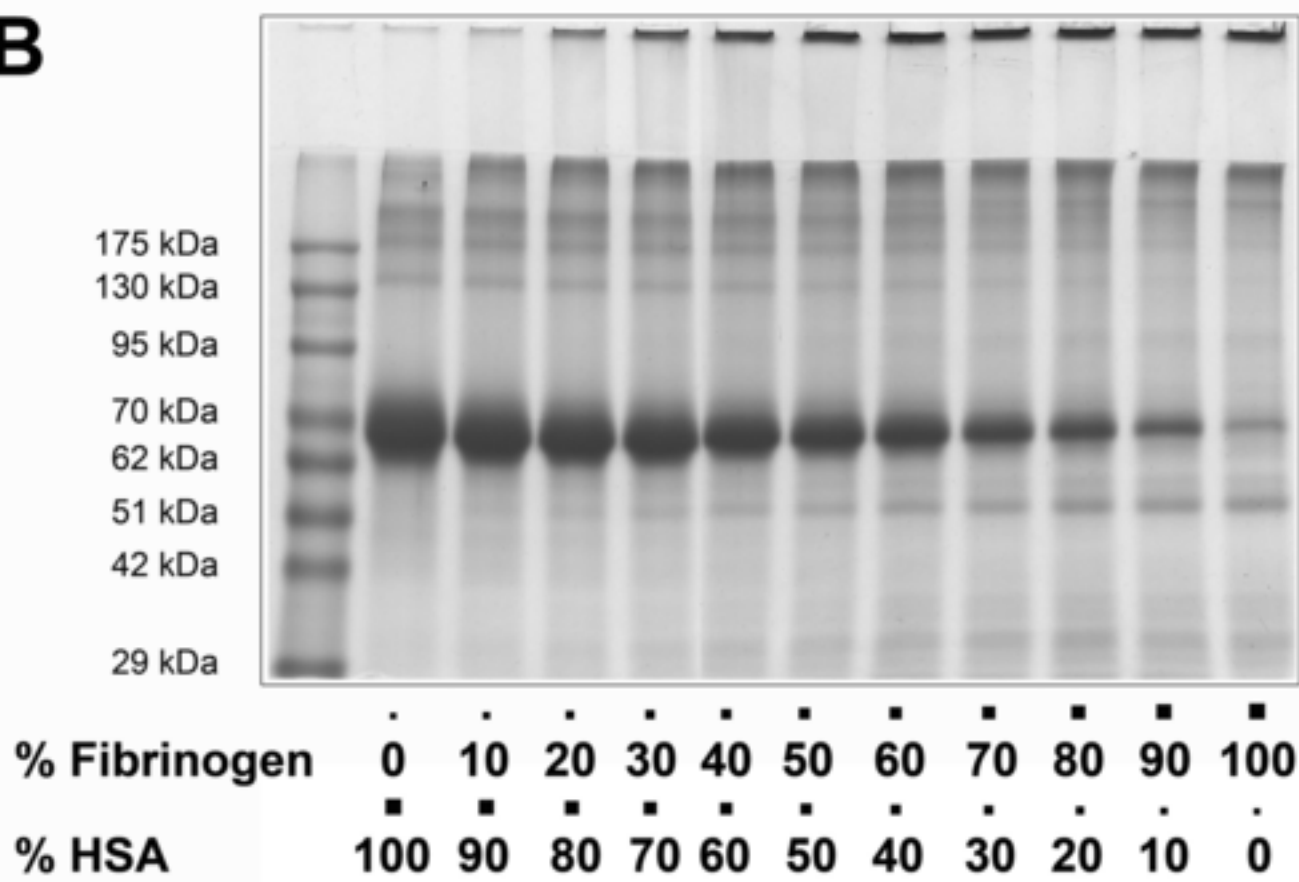


Figure 7

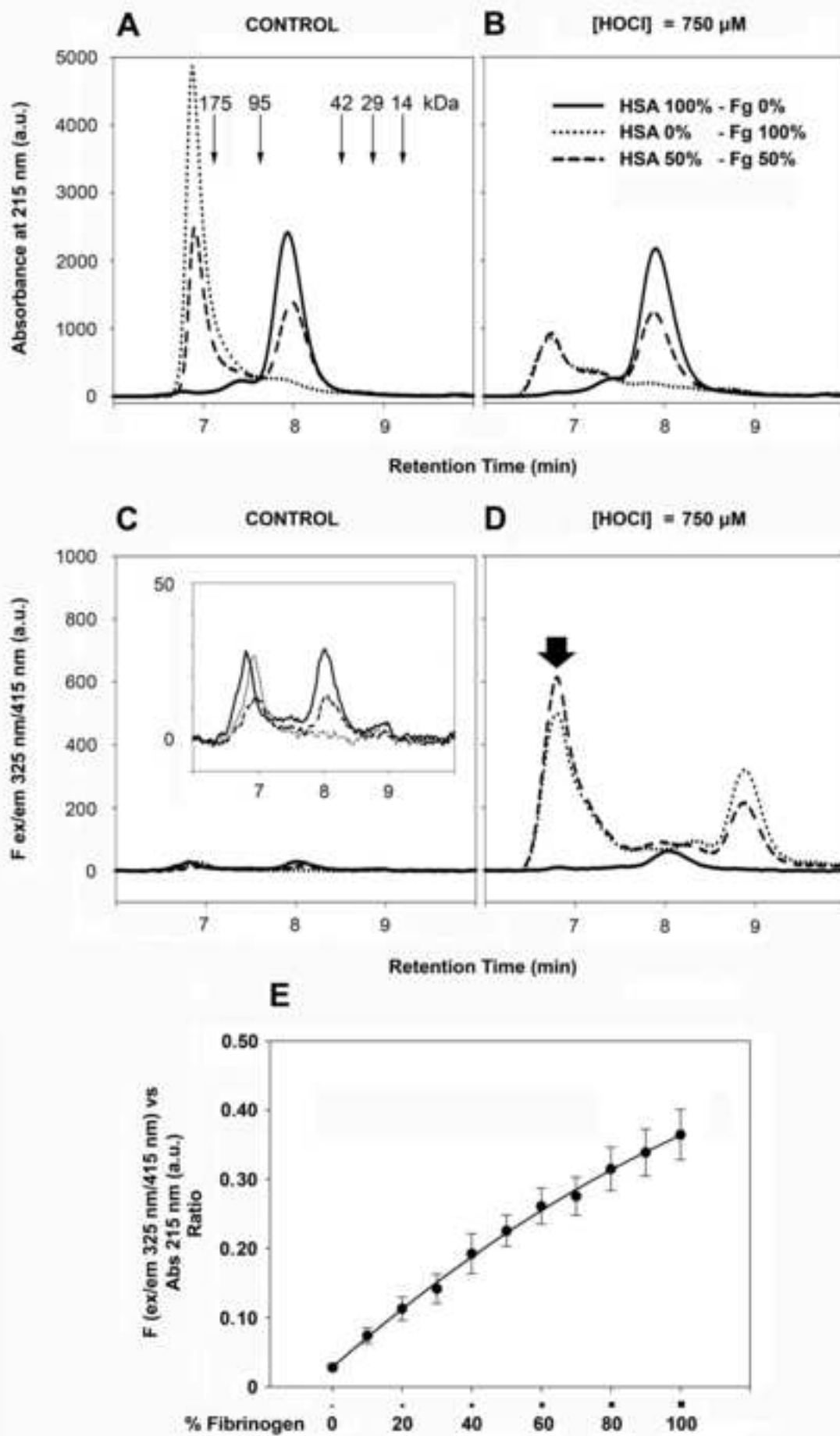


Figure 8

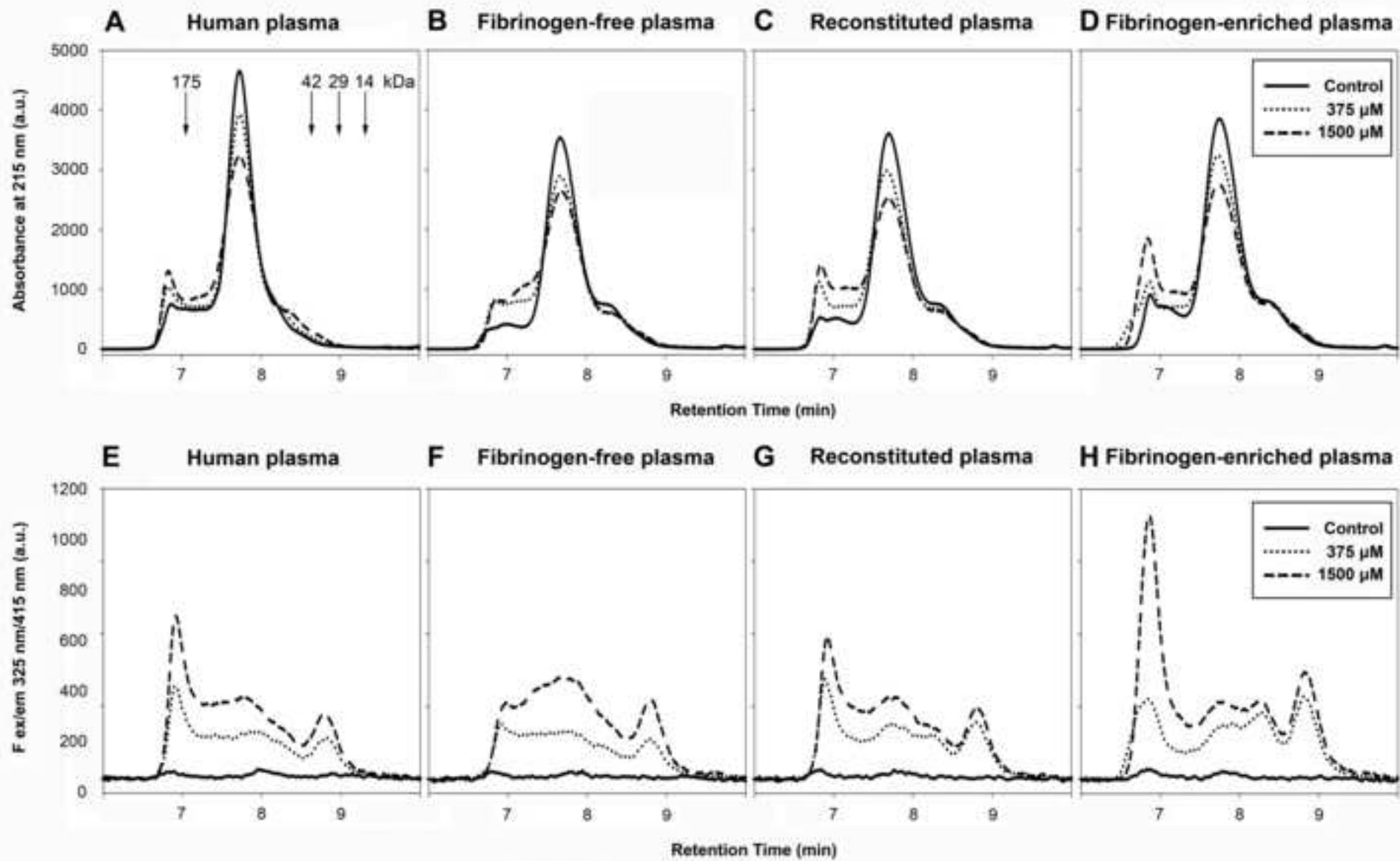


Figure 9

